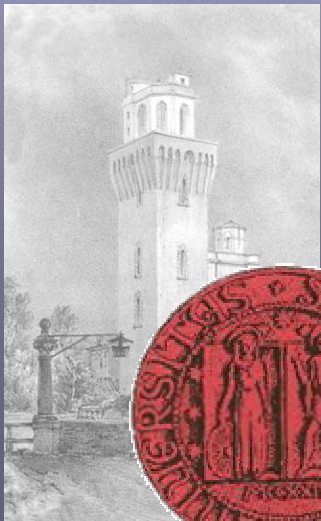


Formation & Evolution of Early Type Galaxies.... and more

Emiliano Merlin & Cesare Chiosi

Astronomy Department, University of Padova, Italy



Highlights - Flashes on Three Questions

- Galaxy formation (ellipticals in particular): hierarchical or monolithic ?
- Continuous or bursting mode of star formation. Which is (are) the key physical cause (s) ?
- Interacting galaxies: can morphology be changed?

Foreword

- ▶ To unravel the formation mechanism & evolutionary history of Elliptical Galaxies (EGs) is one of the challenges of modern astrophysics.
- ▶ Hierarchical or Monolithic? Or a complex mixture of both (revised monolithic)?

Introduction

- Hierarchical: EGs (the massive ones) are the end product of subsequent mergers of smaller sub-units over time scales almost equal to the Hubble time.
- Monolithic: EGs form at high redshift by rapid collapse and undergo a single, prominent star formation episode ever since followed by quiescence.
- Revised Monolithic: a great deal of the stars in massive EGs are formed very early-on at high redshifts and the remaining ones at lower redshifts.

Pros and Cons

- Hierarchical: some evidence that the merger rate likely increases proportional to $(1+z)^3$ together with some hints for a color-structure relationship for E & S0 galaxies (the colors get bluer at increasing complexity). The many successful numerical simulations of galaxy encounters. However the number of EGs does not seem to decrease with the redshift.
- Monolithic: the observational properties of the stellar content in EGs that strongly hints for old and homogeneous stellar populations
- Revised Monolithic: some evidence of star formation at low redshifts indicated by the presence of [OII] lines, the narrow band indices and also the nearly constant number frequency of early type galaxies up to $z=1$ (and above).

Scale Relations

Faber-Jackson

$$L \propto \sigma_0^4$$

Effective Radius- Surface Brightness

$$R_e \propto I_e^{-0.83}$$

Fundamental Plane

$$R_e \propto \sigma^{1.36} I_e^{-0.85}$$

Diameter ($m=20.75 \text{ mag/sec}^2$) -
velocity dispersion - surface brightness

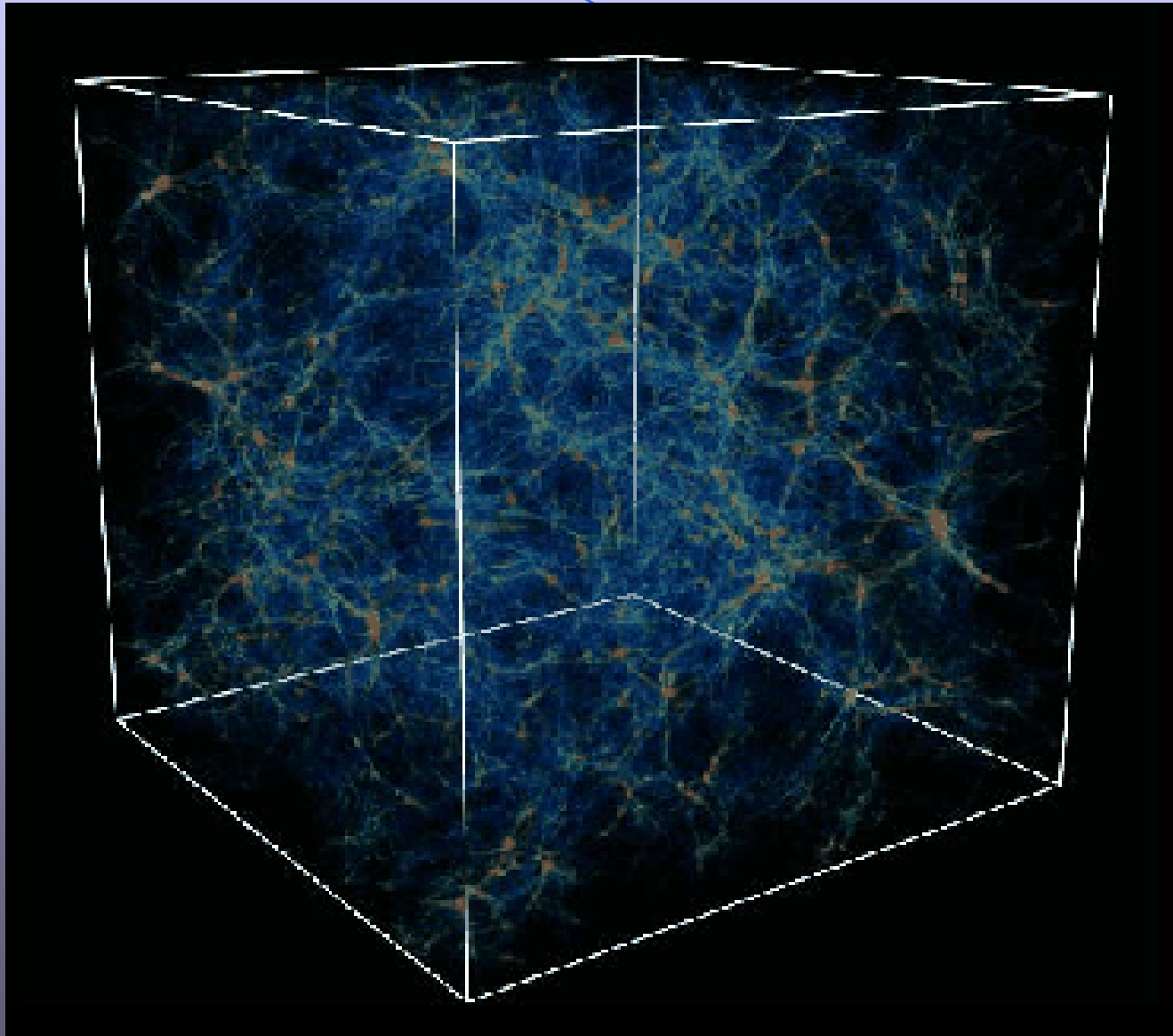
$$D_n \propto \sigma_0^{1.4} I_e^{0.07}$$

Color-Magnitude

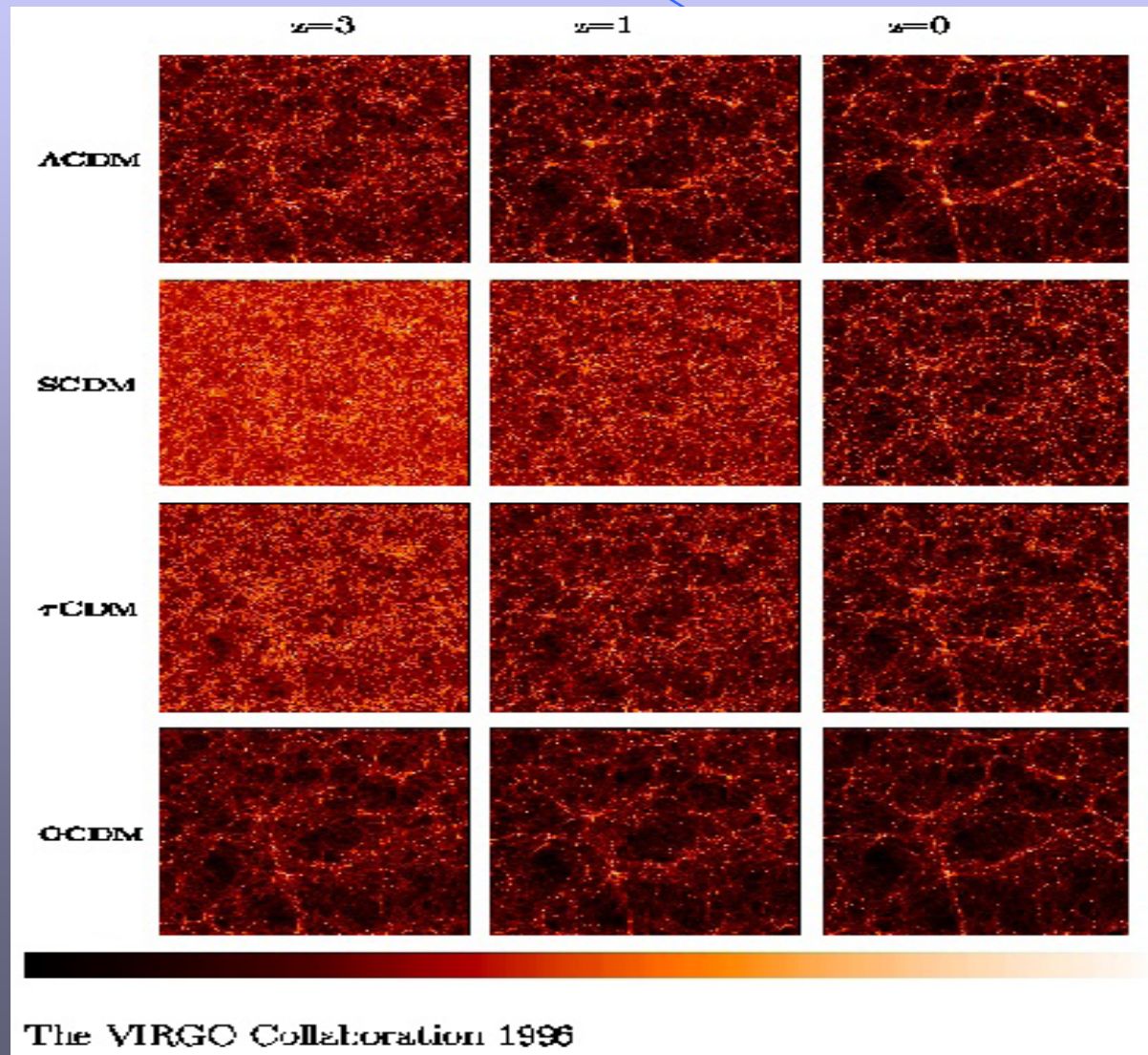


Galactic Winds

Cosmological Simulations

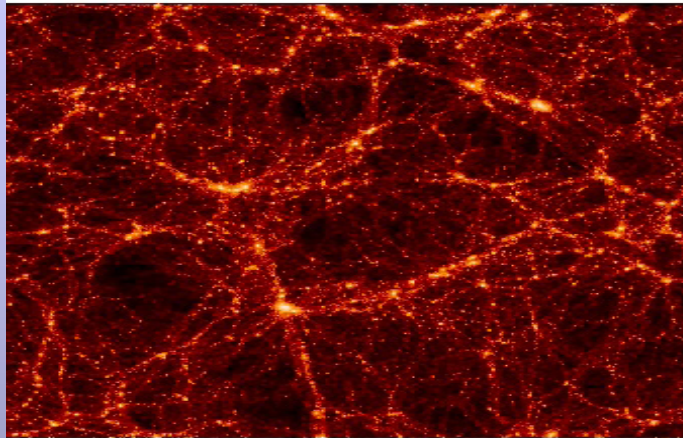


Cosmological Initial Conditions

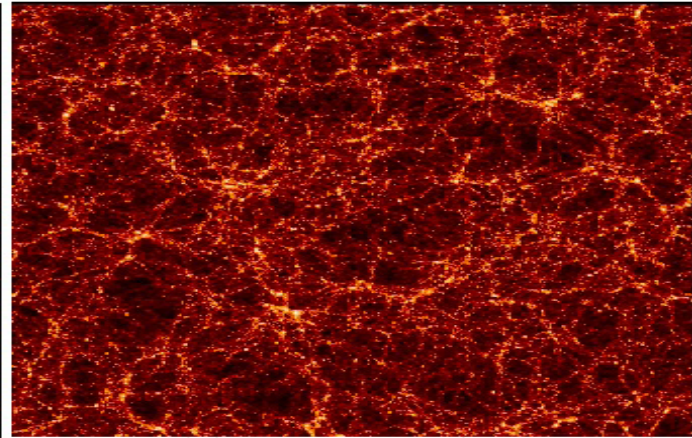


Simulations at $z=0$

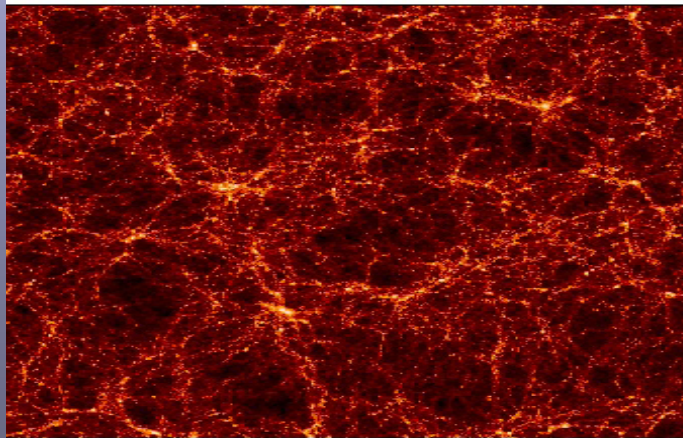
$z=0$



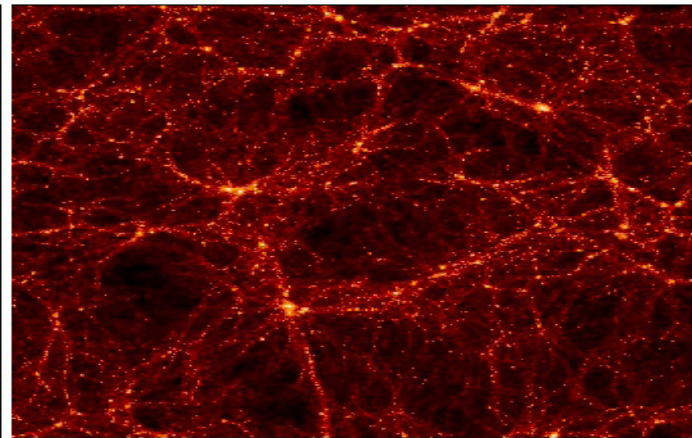
Λ CDM



SCDM



τ CDM

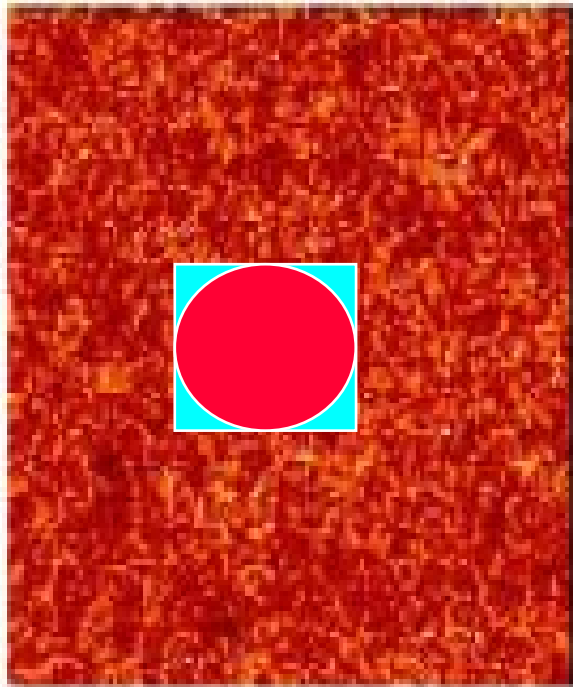


OCDM

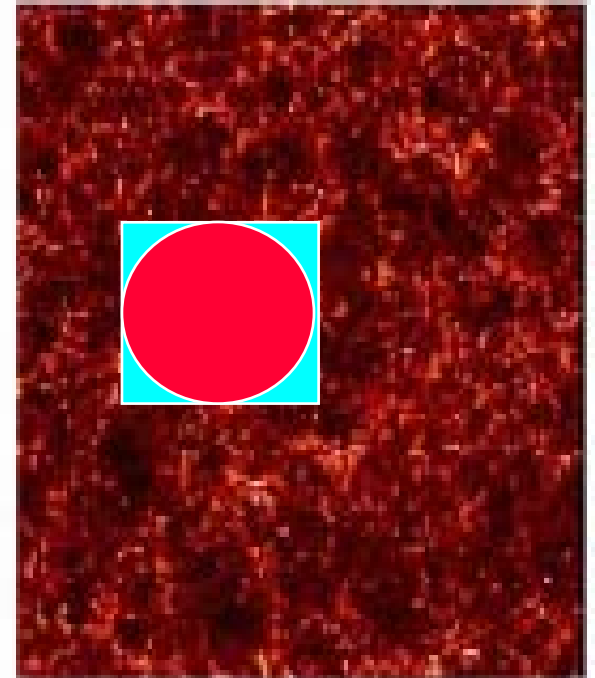
Cut a cube of edge a

Cosmological simulations from GRAFIC2. Isolate an overdense region with peak at the center of cube of edge a (roughly where overdensity $\rightarrow 0$). Derive the geometrical center of the cube.

SCDM



Λ CDM



Cut a sphere of radius $a/2$

Continue

The sphere volume is about half the cube volume and contains about half of the particles of the cube volume.

Choosing the geometrical center instead of the mass-center as origin of a new system of coordinates, overdense regions may happen to be not located at the center.

Distances provided by *GRAFIC2* are referred to the new coordinate system and translated into proper distances (in Mpc)

$$d_{pr} = a_{start} \times r_{comoving}$$

Velocities are referred to the center of the sphere subtracting the velocity as a whole. Then to each particle we add the velocity of the Hubble flow

$$v_{flow} = H(z) \times d_{pr}$$

Continue

In order to calculate $H(z)$ we need to assume a cosmological model

$$H(z) = H_0 \sqrt{\Omega_m (1+z)^3 + \Omega_\Lambda}$$

H_0 , Ω_m and Ω_Λ are the Hubble constant, the matter density, and the dark energy density at the present time (with Λ the Cosmological constant).

Then we add rigid rotation whose spin parameter λ is given by

$$\lambda = \frac{J |E|^{1/2}}{GM^{5/2}}$$

Where J is the angular momentum, E is the initial binding energy and M the total mass of the system. Typical values for λ range from 0.02 to 0.08 \rightarrow angular velocities of the order of fractions of complete rotation over times scale of about $10 \tau_{\text{ff}}$

Comparing with the Chiosi & Carraro (2002) initial Conditions

They start with a spherical model containing Dark and Baryonic Matter (DM and BM, respectively) in cosmological proportions (9:1).

Set the initial density profile of DM according to

$$\rho(r) = \rho_c \frac{r_c}{r}$$

which in the central regions mimics the Navarro, Frenk & White (1996) profile.

Continue

The spatial positions of DM particles are derived from MonteCarlo deviations from the density law.

The initial velocities of DM particles are derived from the velocity dispersion $s(r)$ assuming equipartition among the three components

$$v(r) = \frac{1}{3}\sigma(r) = \sqrt{\rho_c r_c G r \ln\left(\frac{R_T}{r}\right)},$$

which is derived from inserting the density profile in the eqn

$$\rho(r)\sigma(r)^2 = \int_r^{R_T} \frac{GM(r')}{r'^2} \rho(r') dr'$$

The gas particles are homogeneously and randomly distributed in the halo of cold DM with null velocity field \rightarrow infall of BM in the potential well of DM.

Continue

This is equivalent to start with a DM halo already detached from the Hubble flow which starts collapsing carrying along BM.

Even if all this sounds reasonable, it already contains the solution of the problem:

The self-gravitating, collapsing Halo of DM has a density profiles already **resembling** the one we are looking for.

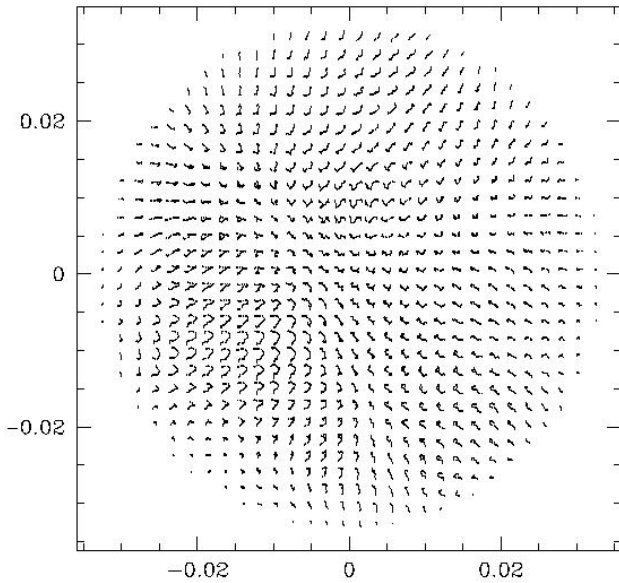
Furthermore, in CDM cosmology the catching up of Baryons by DM happens at much earlier times than the time at which the proto-galactic halo detaches from the Hubble flow.

The initial radius of the protogalaxy is from the mean density of the Universe

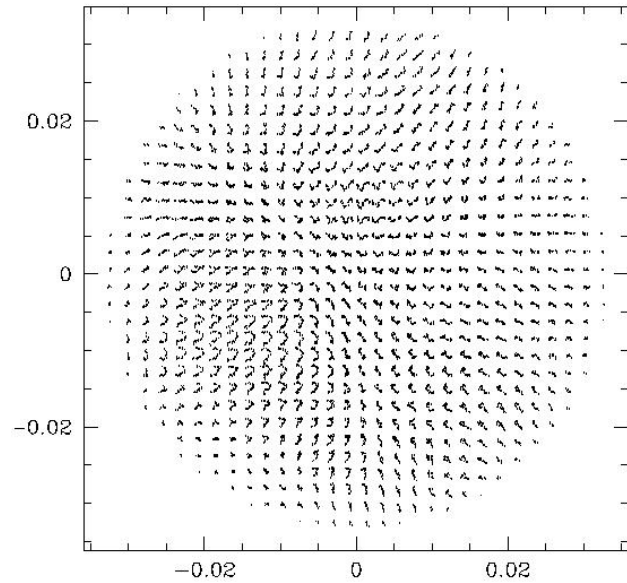
$$\rho_u(z) = \frac{3H_0^2}{8\pi G}(1+z)^3$$

Initial Models: Positions

DM



Gas

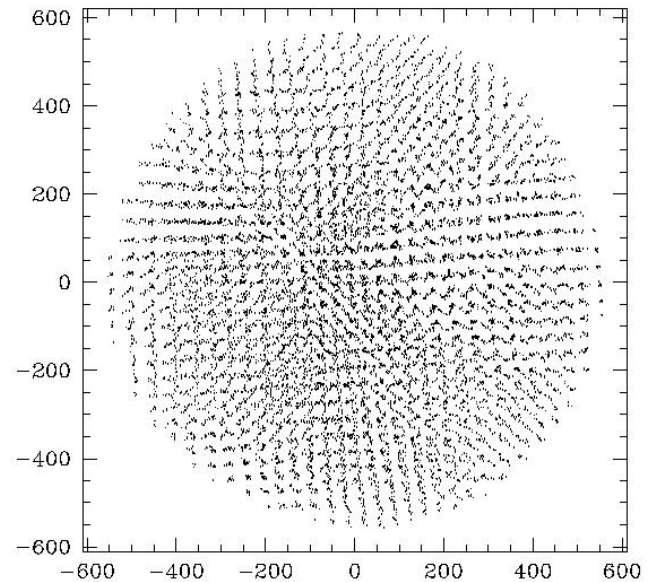
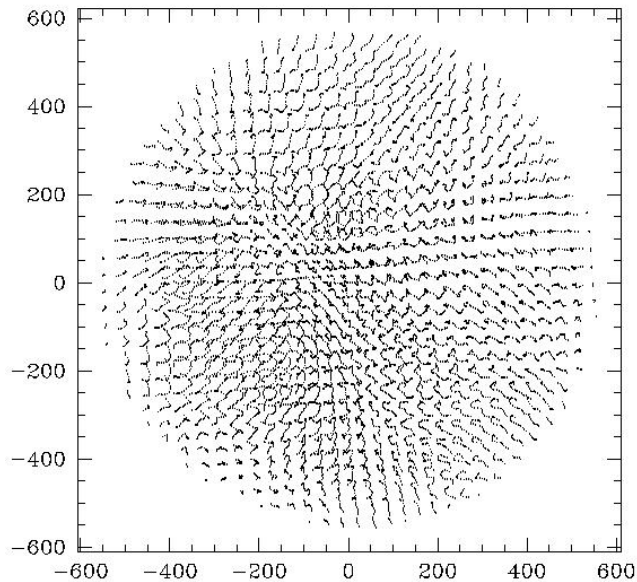


Proper Mpc

Initial Models: Velocities

DM

Gas



Km/s

Basic Physics of Galaxy Models

- Fundamental equations
- Cooling
- Star formation and initial mass function
- Heating
- Chemical enrichment
- N-body-TSPH

Fundamental Equations

$$\frac{d\rho}{dt} = -\rho\nabla v$$

$$\frac{dv}{dt} = -\frac{1}{\rho}\nabla P - \nabla\Phi$$

$$\frac{du}{dt} = -\frac{P}{\rho}\nabla u + S$$

$$\nabla^2\Phi = 4\pi G\rho$$

Continuity

Momentum

Energy

Gravitational Potential

$$S = \frac{\Lambda - \Gamma}{\rho}$$

Source function: Λ and Γ are the heating and cooling rates

Cooling

Radiative Cooling

$$\tau_{cool} = E \left(\frac{dE}{dt} \right)^{-1} \approx \frac{3\rho kT}{2\mu\Gamma(T)}$$

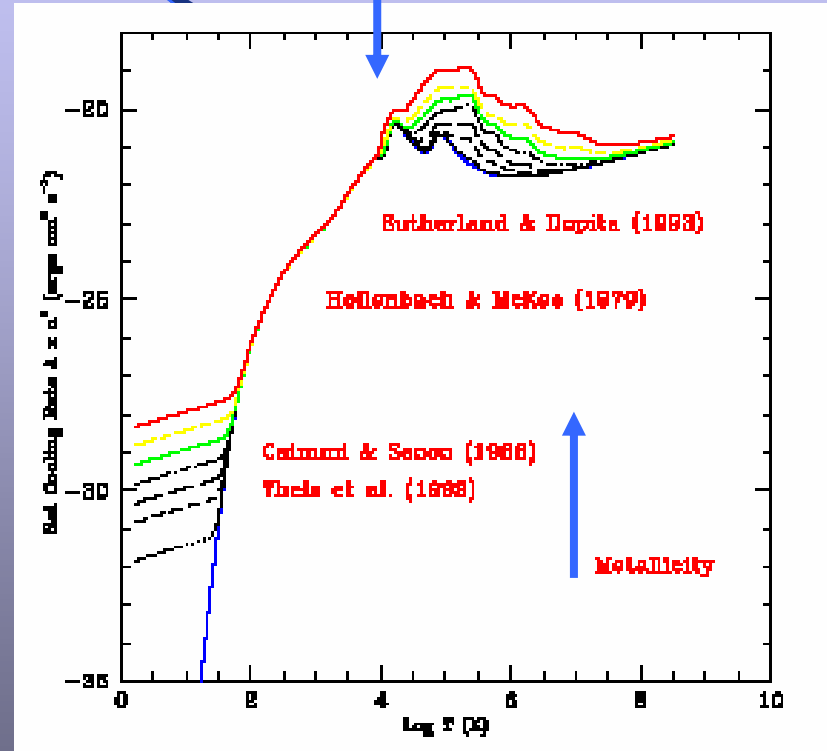
with $\Gamma(T)$ the cooling rate

Compton Cooling

$$\Gamma_{comp} = \frac{4\sigma_T n_e \rho_R (T - T_R)}{m_e}$$

with cooling time

$$\tau_{cool} = \frac{[3m_p m_e (1+z)^{-4}]}{8\mu\sigma_T \Omega_R \rho_c} \approx \tau_{dyn} = \left(\frac{2GM}{R^3} \right)^{0.5}$$



Taken into account at high z

Star Formation Rate & Initial Mass Function

$$\frac{d\rho_*}{dt_g} = -\frac{d\rho_g}{dt_g} = c^* \frac{\rho_g}{t_g}$$

The Schmidt law

$$\begin{aligned}\Phi_S(M) &= C_S M^{-1.35} && \text{Salpeter} \\ \Phi_K(M) &= \begin{cases} C_{K1} M^{-0.5} & \text{if } M < 0.5 \\ C_K M^{-1.2} & \text{if } 0.5 < M < 1 \\ C_K M^{-1.7} & \text{if } M > 1 \end{cases} && \text{Kroupa} \\ \Phi_A(M) &= C_A M^{-1.00} && \text{Arimoto \& Yoshii} \end{aligned} \quad (23)$$

$$C_S = 0.17$$

$$C_{K1} = 0.48$$

$$C_K = 0.29$$

$$C_A = 0.14$$

→ Adopted

Heating

Total heating rate by radiative processes is

$$H_R = \frac{E_{SNI} + E_{SNII} + E_w + E_{UV}}{\Delta t}$$

Heating by Type I & Type II SN. Winds and UV neglected

$$E_{SNI,II} = \int_{\Delta t} \epsilon_{SNI,II} r_{SNI,II}(t') dt'$$

Where $\epsilon_{SNI,II}$ is the energy liberated by a single explosion, and $r_{SNI,II}$ is the rate of SN production per time interval Δt

Chemical Enrichment

At the end of its life star of mass M ejects the total amount of metals

$$M_Z = y_Z M + z_0 (M - M_r)$$

The fractionary mass of metals given by a SSP at time t is

$$E_Z = \int_{M(t)}^{M_u} \frac{M_Z}{M} \Phi(M) dM$$

The rate of metal injection is

Y_Z are from Portinari et al. (1998) And Marigo (2001). See Lia et al (2002) for details.

$$e_Z(t) = p_Z(t) + Z_0 e(t) \quad \text{where}$$
$$e(t) = \left[\frac{M - M_r(M)}{M} \Phi(M) \left(-\frac{dM}{d\tau} \right) \right]_{M(t)} \quad \text{and}$$
$$p_Z(t) = \left[y \frac{\Phi(M)}{M} \left(-\frac{dM}{d\tau} \right) \right]_{M(t)}$$

Add contribution by SNIa and apply TSPH

Need explosion rate (see above) and amounts of metals ejected per explosion (Iwamoto et al. 1999)

The total amount of metals ejected by a SSP is

$$p_Z^{Tot}(t) = p_Z(t) + M_Z^{SNI} \times R_{SNI}(t)$$

Apply TSPH diffusion among particles

$$\frac{dZ}{dt} = -k \nabla^2 Z$$

Diffusion coefficient from Thornton et al. (1998)

A Few Words on the PD N-Body-TSPH Code

Fully lagrangian N-Body code: Tree-Code for gravity
SPH formalism for fluid experiencing
heating, cooling, chemical enrichment...

Fluid elements represented by a finite number of particles, smoothing required to smear local fluctuations. Any physical quantity $f(r)$ over a finite interval is derived from a Kernel W (peaking at $r=0$)

$$\langle f(r) \rangle = \int W(r - r', h) f(r') dr'$$

where h is the smoothing length, which gives the volume over which the space average is made.

Continue

For $f(r)$ we use the gather/scatter function (Henquist & Katz 1989)

$$\langle f(r) \rangle = \int f(r') \frac{1}{2} [W(r-r', h(r')) + W(r-r', h(r))] dr'$$

For W we adopt Monaghan & Lattanzio (1985)

Add to the Euler equation a term for viscosity in order to describe processes more complicated than shock waves (Monaghan & Lattanzio 1985).

Derive the particle velocities with the so-called leap-frog method

Derive the time-step of each gas particle Courant-Katz condition.

Derive the gravitational acceleration from the quadrupole moment of the gravitational potential (the softening parameter comes in).

Probabilistic Description of Star Formation, Heating & Chemical Enrichment

Following Lia et al (2002) we adopt the probabilistic description for star formation, gas restitution, stellar feed-back, and chemical enrichment.

For instance, the Schmidt law of star formation is interpreted as the probability that at each time step a gas particle is instantaneously and fully turned into a star particle.

Similarly for gas restitution, stellar feed-back and enrichment.

Advantage is that the number of baryonic particles can be kept constant. Save lots of computing time.

Galaxy Models: the Parameters

The cosmological initial conditions (Table 1)

The initial dynamical and computational parameters (Table 2)

The Cosmological Parameters

Table 1. Initial parameters for Models SA, SB and L. S-CDM stands for Standard CMD

Model	SA	SB	L
Cosmological Background	S-CDM	S-CDM	Λ -CDM
Initial redshift	50	53	60
Ω_m	1	1	0.27
Ω_Λ	0	0	0.73
$H_0 = 50 \text{ kmMpc}^{-1} \text{ s}^{-1}$	50	50	71
σ_8	0.5	0.5	0.84

Dynamical and computational parameters

Table 2. Initial dynamical and computational parameters for Models SA, SB and L.

Model	SA	SB	L
Initial number of gas particles	13719	13904	13707
Initial number of CDM particles	13685	13776	13657
Initial total mass ($10^{12} M_{\odot}$)	1.62	0.03	0.88
Initial baryonic mass fraction	0.10	0.10	0.16
Initial radius (kpc)	33	9	27
Softening parameter for gas (kpc)	1	0.5	1
Softening parameter for DM (kpc)	2	1	2

Results: Model SA

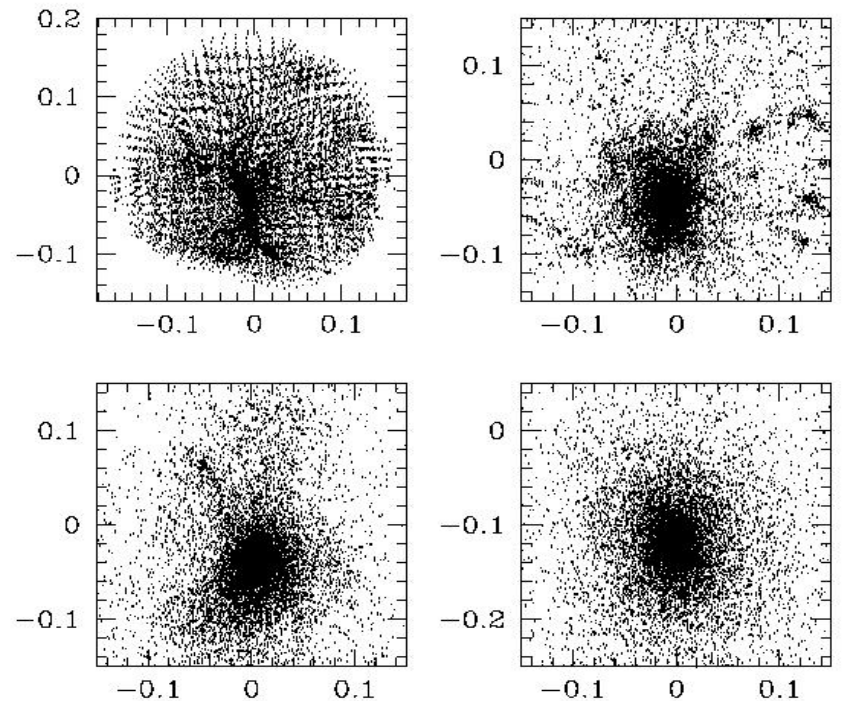
Model SA

Dark Matter

Projection onto
the XY plane

Coordinates in
proper Mpc

From top to bottom
and left to right
 $Z=7.6, 3.2, 1.6, 0$



Results: Model SA

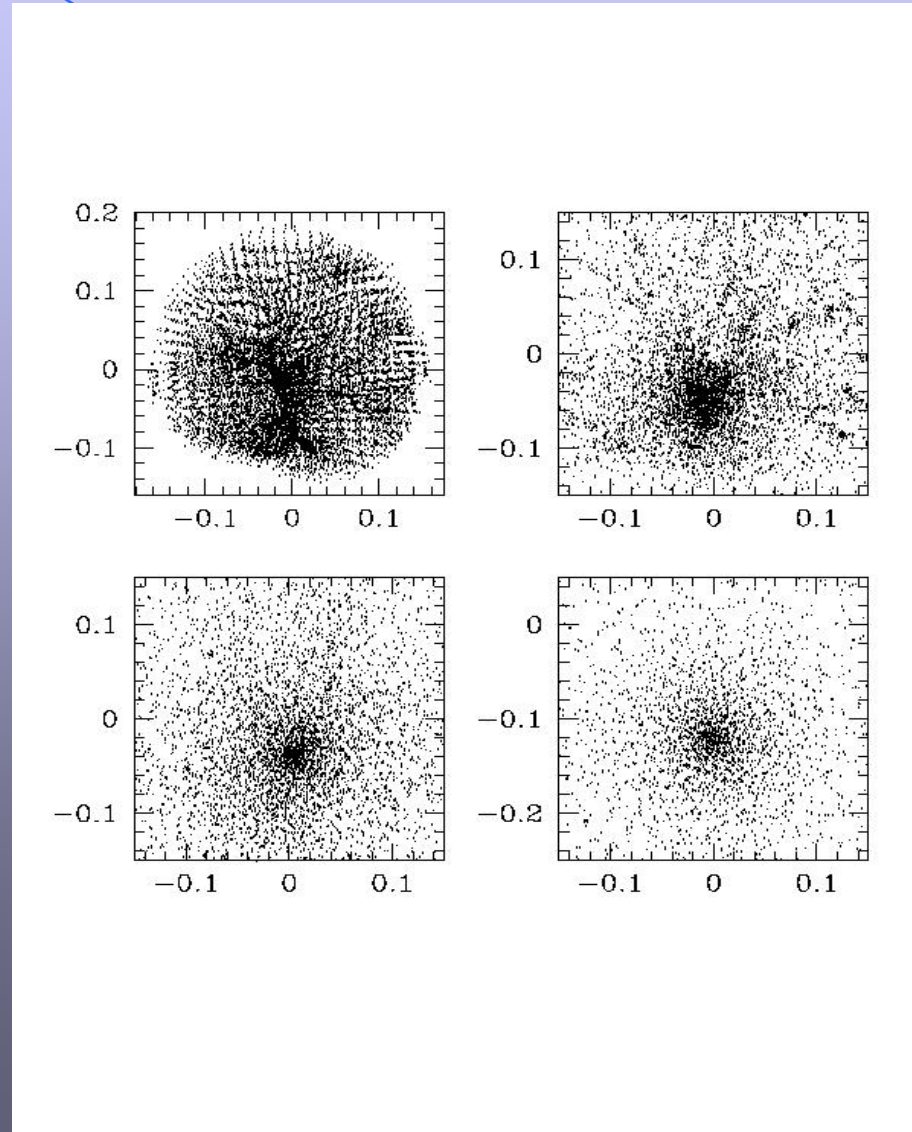
Model SA

Gas

Projection onto
the XY plane

Coordinates in
proper Mpc

From top to bottom
and left to right
 $Z=7.6, 3.2, 1.6, 0$



Results: Model SA

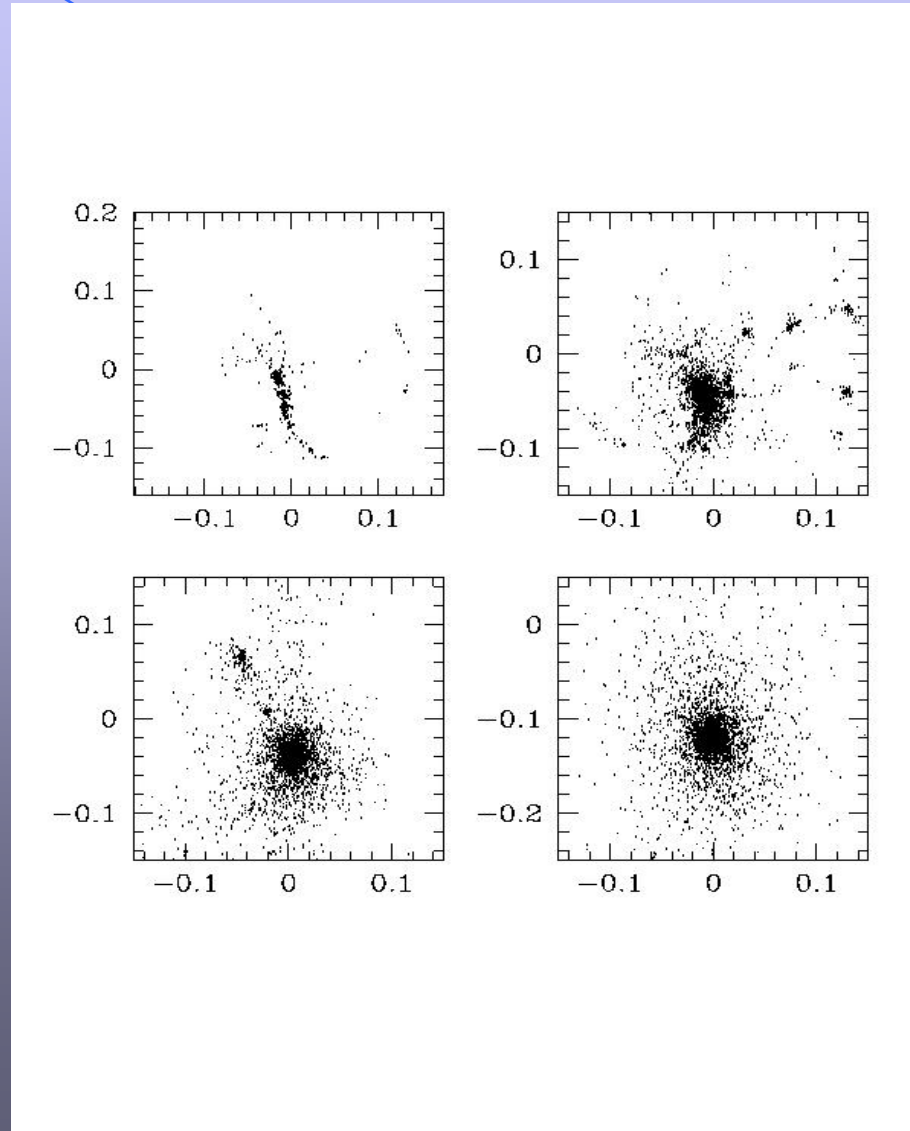
Model SA

Stars

Projection onto
the XY plane

Coordinates in
proper Mpc

From top to bottom
and left to right
Z=7.6, 3.2, 1.6, 0



Results: Model SB

Model SB

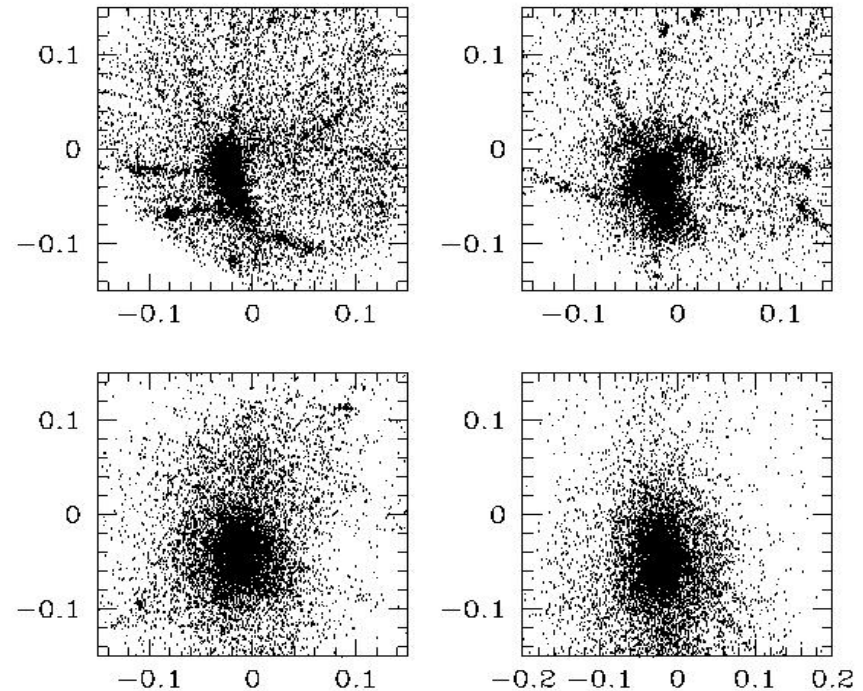
Dark Matter

Projection onto
the XY plane

Coordinates in
proper Mpc

From top to bottom
and left to right

$Z=6.3, 4.2, 2.2, 1.0$



Results: Model SB

Model SB

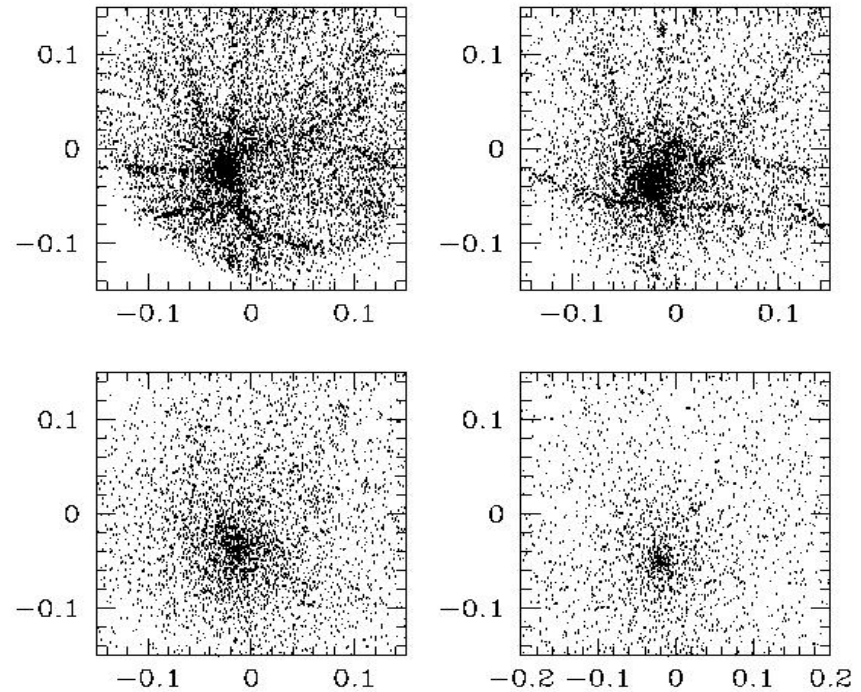
Gas

Projection onto
the XY plane

Coordinates in
proper Mpc

From top to bottom
and left to right

$Z=6.3, 4.2, 2.2, 1.0$



Results: Model SB

Model SB

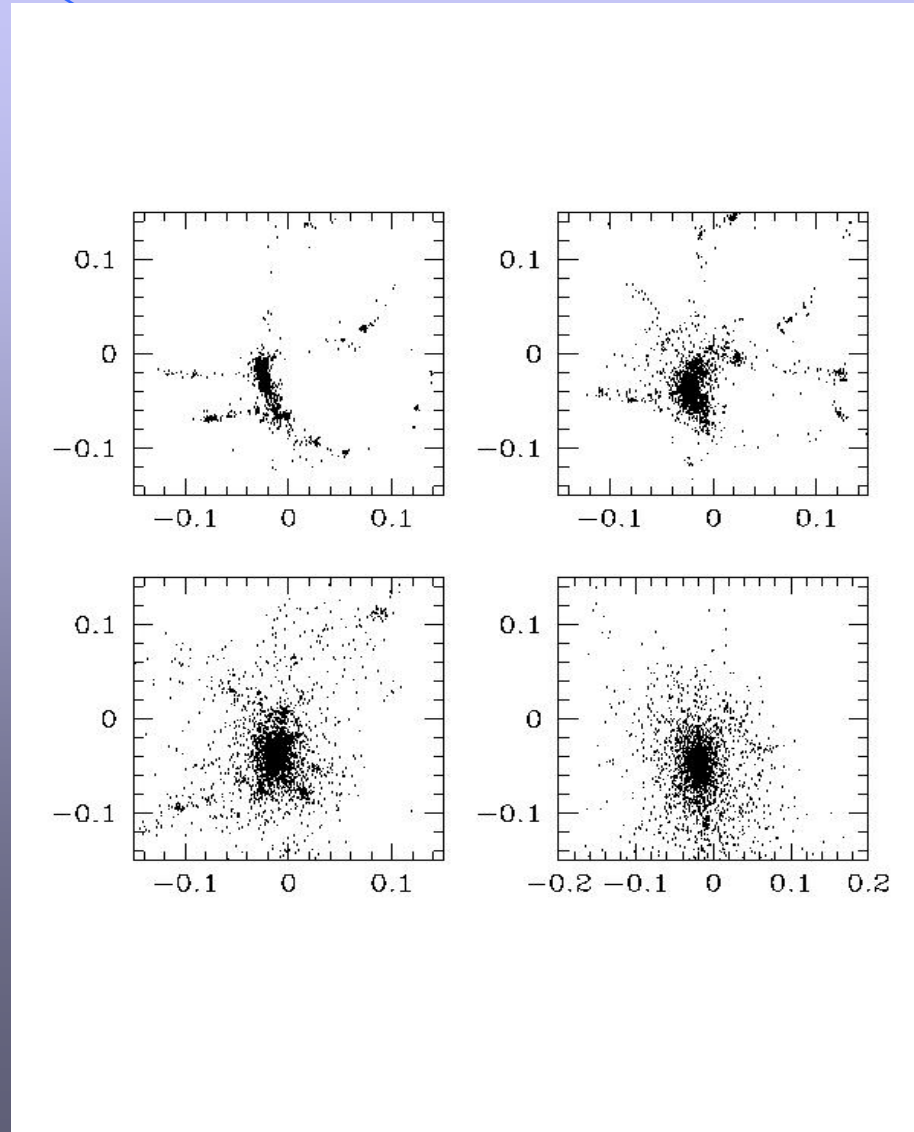
Stars

Projection onto
the XY plane

Coordinates in
proper Mpc

From top to bottom
and left to right

Z=6.3, 4.2, 2.2, 1.0



Results: Model L

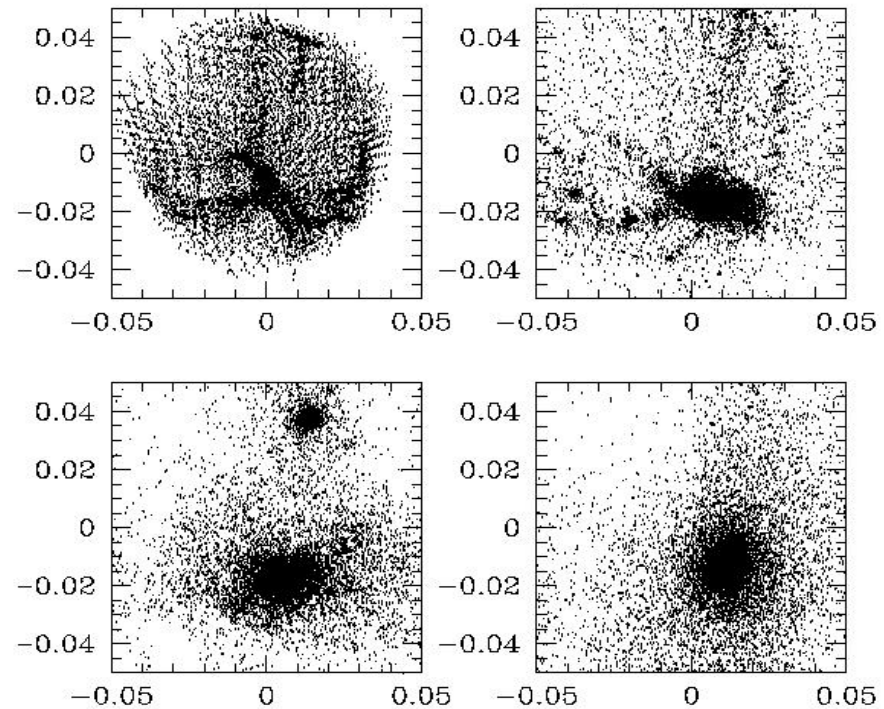
Model L

Dark Matter

Projection onto
the XY plane

Coordinates in
proper Mpc

From top to bottom
and left to right
 $Z=7.5, 3.9, 2.0, 0.9$



Results: Model L

Model L

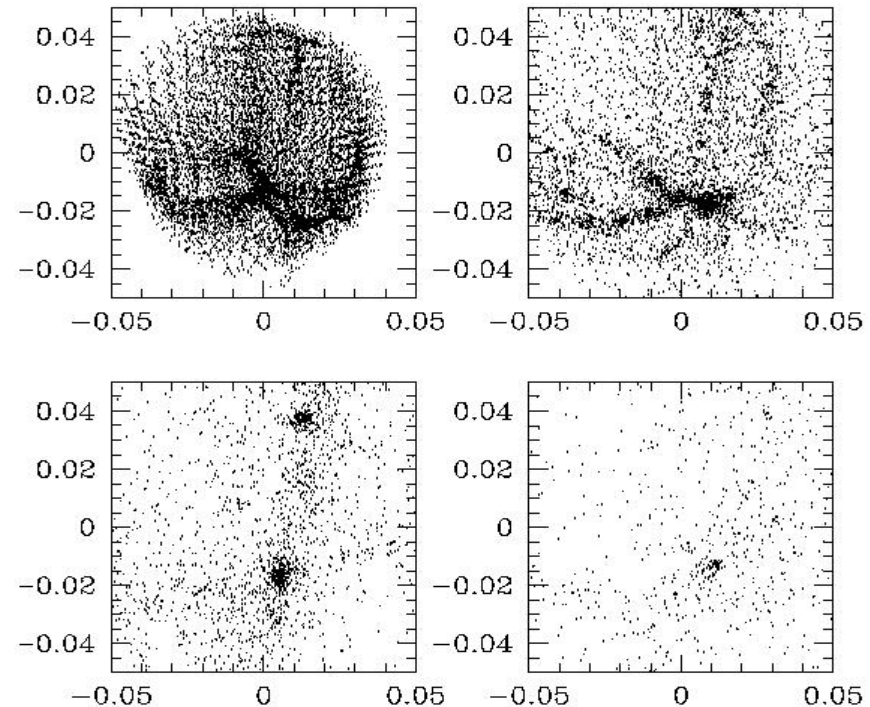
Gas

Projection onto
the XY plane

Coordinates in
proper Mpc

From top to bottom
and left to right

$Z=7.5, 3.9, 2.0, 0.9$



Results: Model L

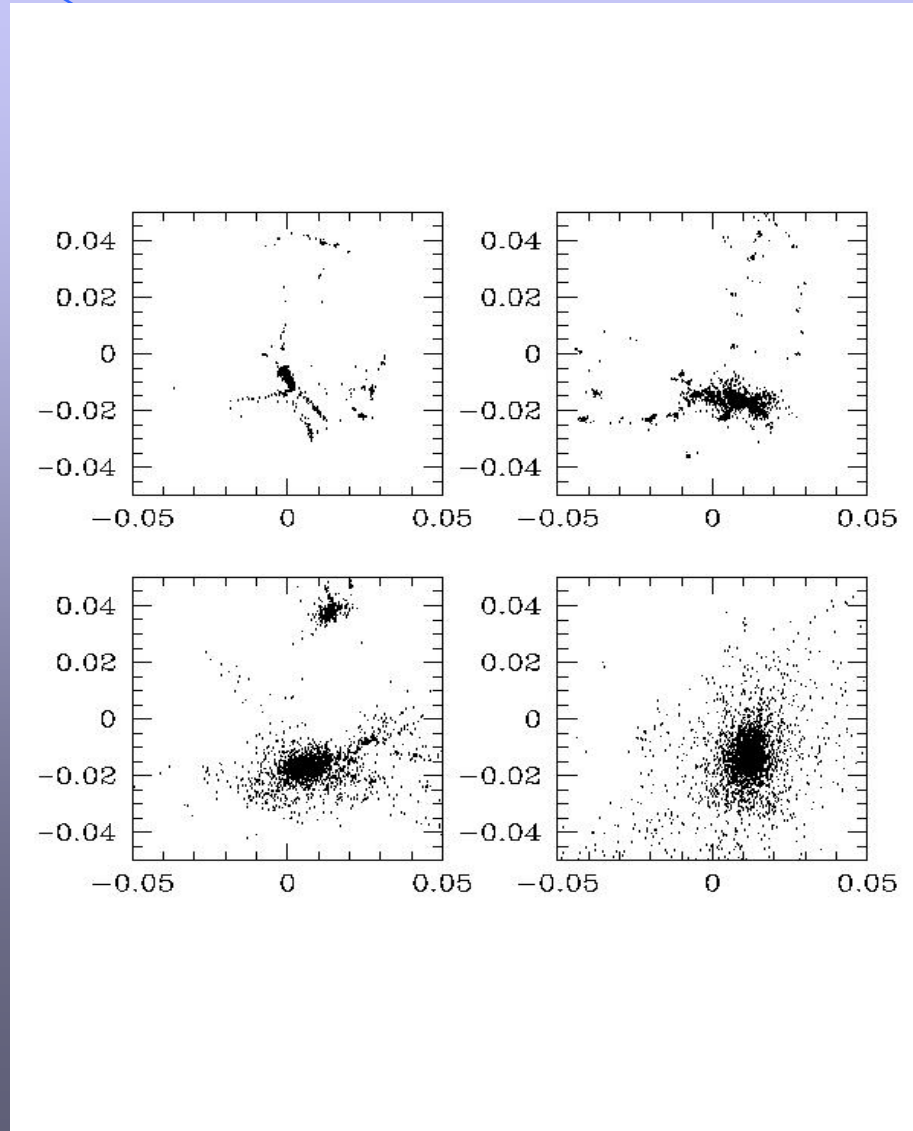
Model L

Stars

Projection onto
the XY plane

Coordinates in
proper Mpc

From top to bottom
and left to right
Z=7.5, 3.9, 2.0, 0.9



Spatial Structure: Axial Ratios

Definition

$$\frac{b}{a} = \sqrt{\frac{\sum m_i y_i^2}{\sum m_i x_i^2}} \quad \frac{c}{a} = \sqrt{\frac{\sum m_i z_i^2}{\sum m_i x_i^2}}$$

Results

<i>Ratio</i>	<i>Stars</i>	<i>Dark</i>	<i>Matter</i>		
$\frac{b}{a}$	1.08		1.14	Model	SA
$\frac{c}{a}$	1.07		1.17		
<i>Ratio</i>	<i>Stars</i>	<i>Dark</i>	<i>Matter</i>		
$\frac{b}{a}$	1.04		1.14	Model	SB
$\frac{c}{a}$	1.00		0.96		
<i>Ratio</i>	<i>Stars</i>	<i>Dark</i>	<i>Matter</i>		
$\frac{b}{a}$	1.17		1.15	Model	L
$\frac{c}{a}$	1.04		1.19		

SA & SB Nearly Spherical
L Has a larger b/a ratio

Dark Matter more asymmetric

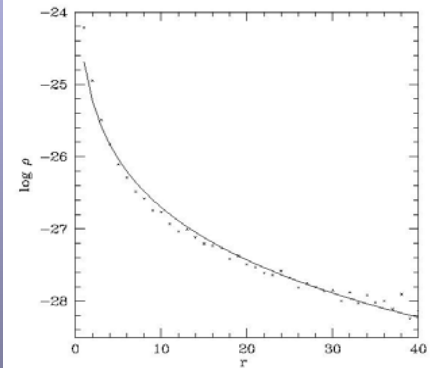
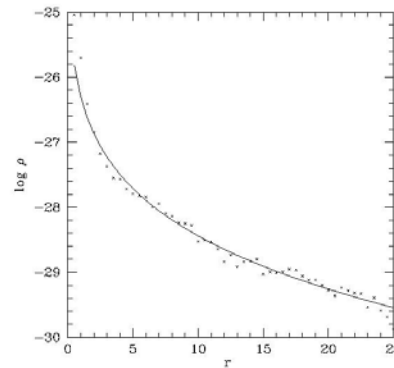
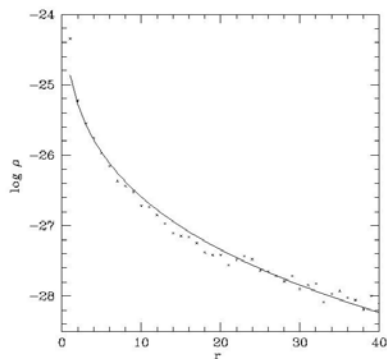
Spatial Structure

SA

SB

L

Stellar densities of models compared with the Sersic Law



$$\Sigma = \Sigma_e \exp[-(0.324 - 2m)] \times \left[\left(\frac{R}{R_e} \right)^{1/m} - 1 \right]$$

Final surface density profiles (projected on XY)

Stellar and Dark Matter profiles

The Hernquist (1990) law for the star density profile; a is the scale length and M the total Mass.

$$\rho(r) = \frac{Ma}{2\pi r} \frac{1}{(r+a)^3}$$

The Navarro, Frenk & White (1996) density profile for DM; ρ_{cri} is the critical density, δ_c is a parameter, R_s is the scale radius.

$$\rho(r) = \frac{\rho_{\text{cri}} \delta_c}{\frac{r}{r_s} \left(1 + \frac{r}{r_s}\right)^2}$$

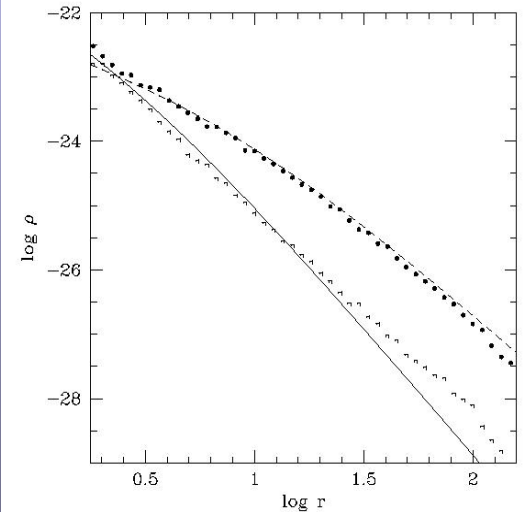
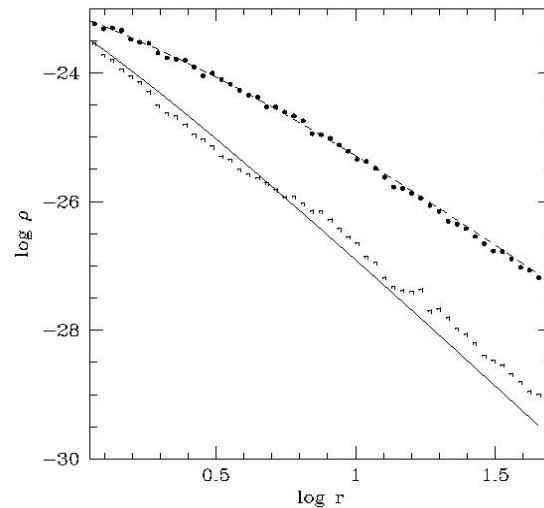
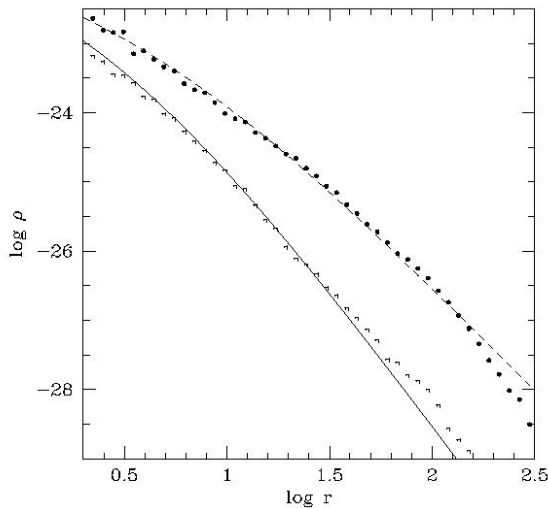
Results: density profiles

SA

SB

L

Dark Matter profile is too steep in the central regions



Final spherical density profiles

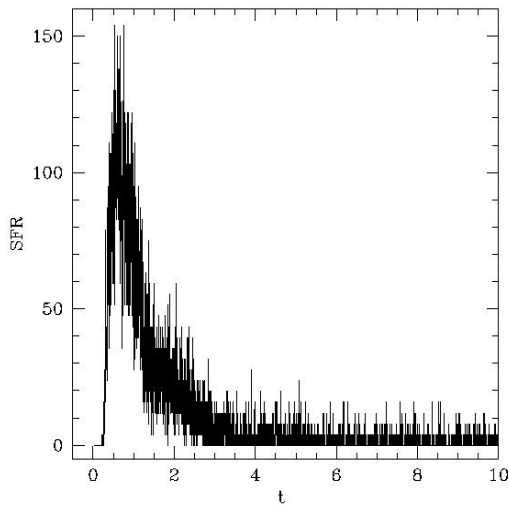
Star Formation History

Table 3. Masses and half mass radii for the various components of Models SA, SB and L; masses are in units of $10^{12} M_{\odot}$, radii are in kpc.

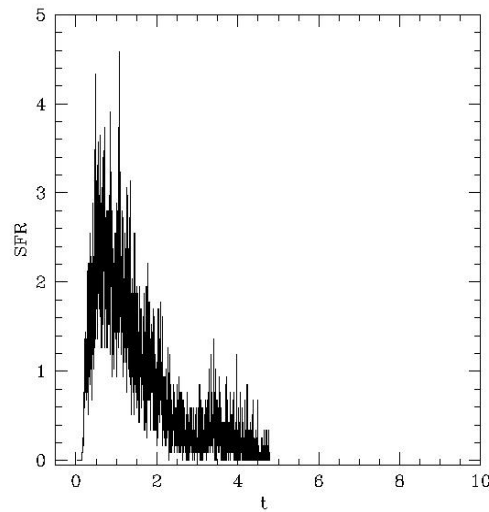
Model	SA	SB	L
Initial Total Mass	1.620	0.035	0.884
Initial Dark Matter mass	1.458	0.0305	0.743
Initial Baryonic mass M_B	0.162	0.0035	0.141
Final gas mass (collapsed)	0.062	0.0004	0.044
Final star mass M_s	0.091	0.0029	0.088
M_s/M_B	0.56	0.82	0.62
Half mass radius of stars	7	1	3
Half mass radius of DM	52	15	44
Age of the last model (Gyr)	13	5	6

Star Formation Rates

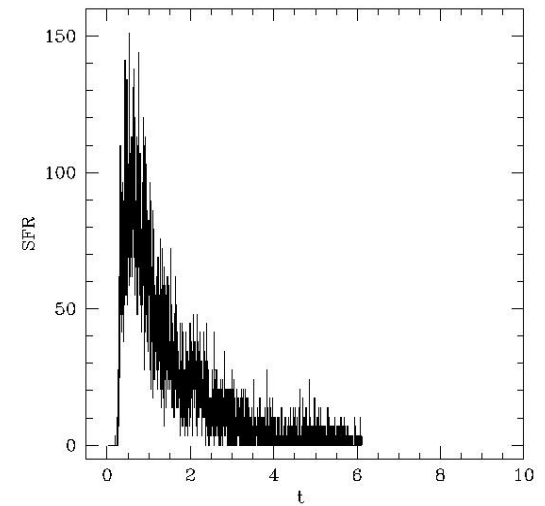
SA



SB



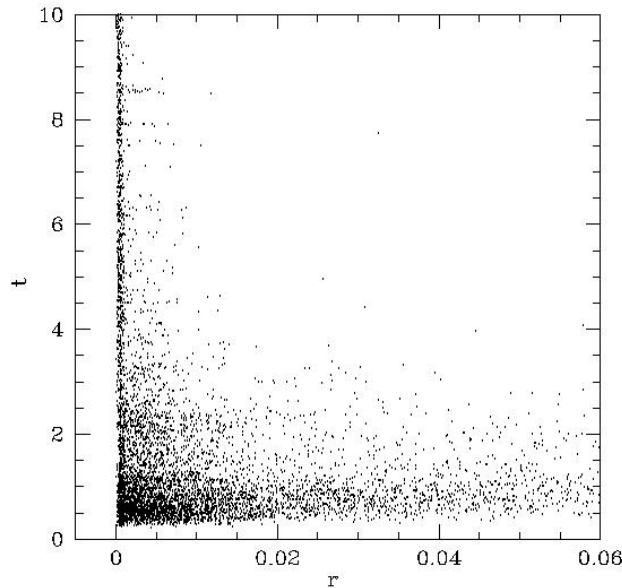
L



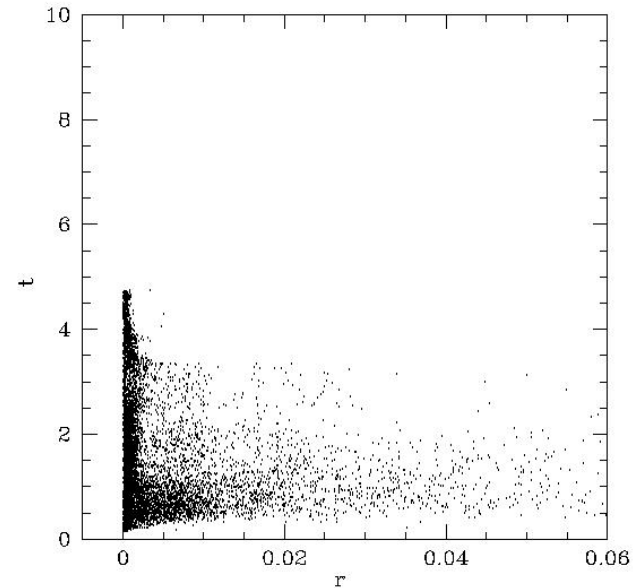
In solar masses per year

Age-radial distance

SA



SB

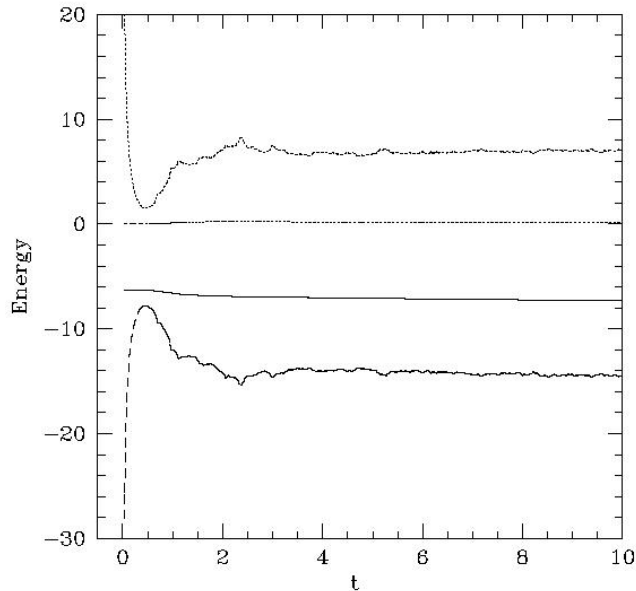


Outward-inward building up of galaxies

Energy Conservation

Model SA

Energies in code units



Legend

Dotted: kinetic energy

Short-dotted: potential energy

Dotted-dashed: thermal energy

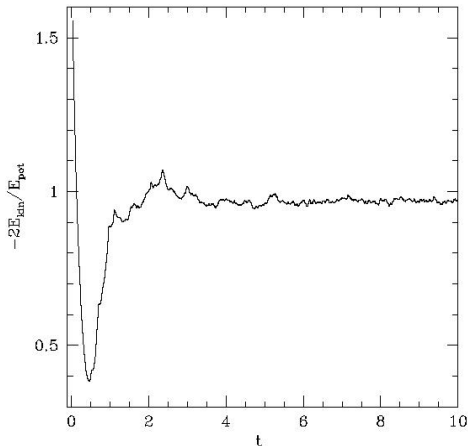
Solid: total energy

Virial Trace

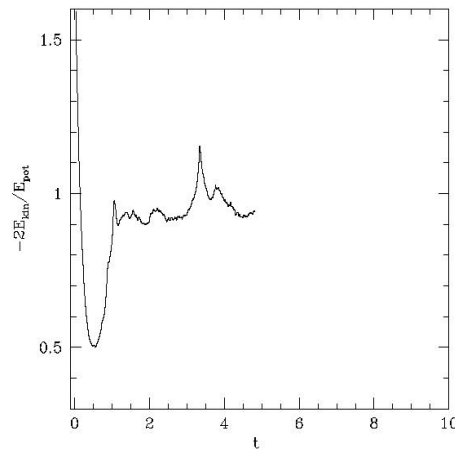
$$\text{Virial Trace} = -2E_{kin} / E_{pot}$$

Models tend to relaxation state

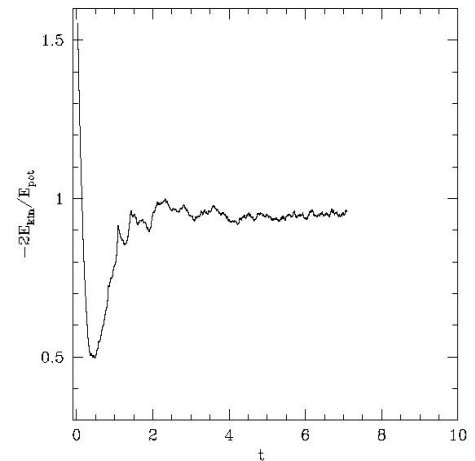
Virial Trace for a fully relaxed system is equal to 1



SA



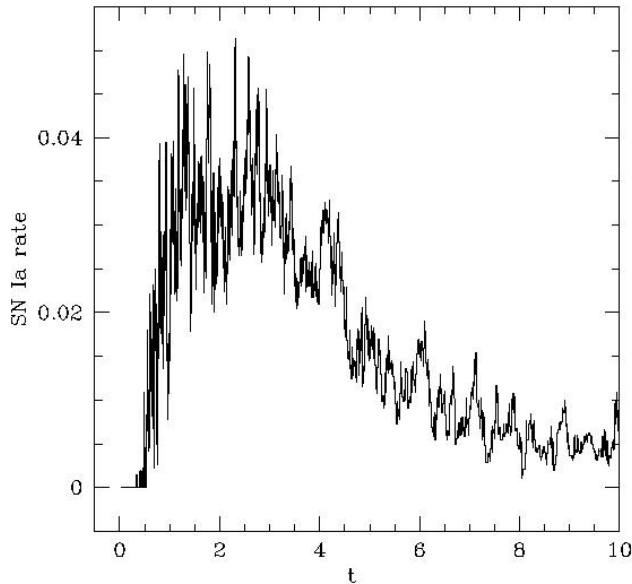
SB



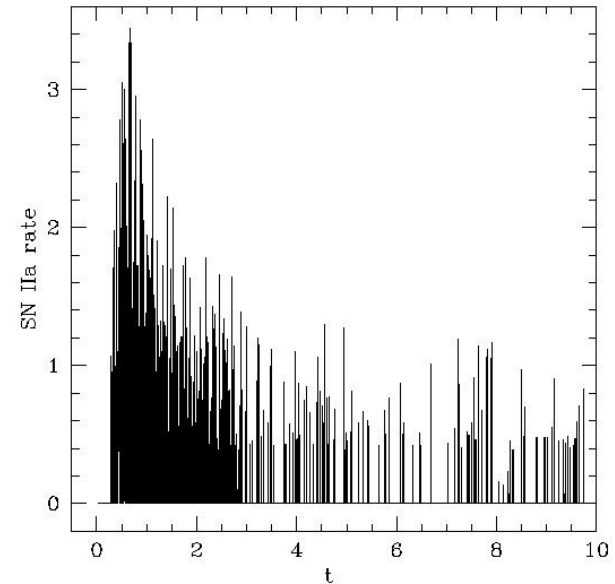
L

Energy Feed-back

Model SA



SN Type Ia



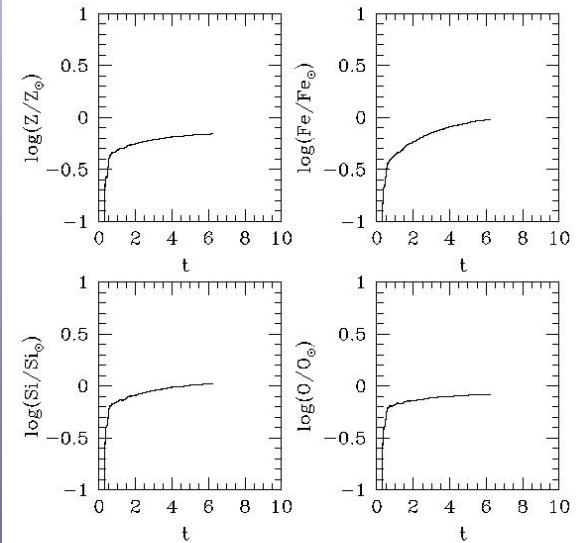
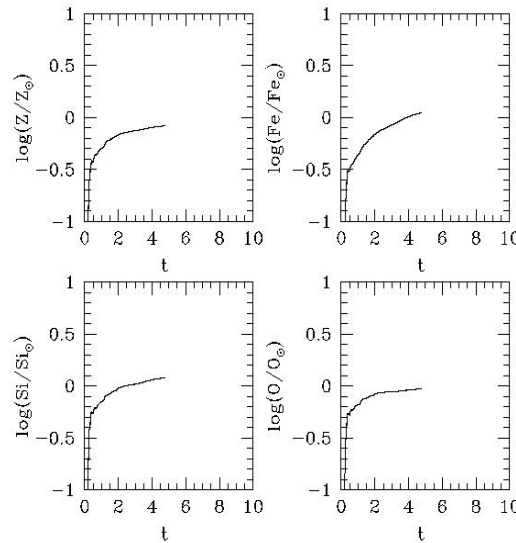
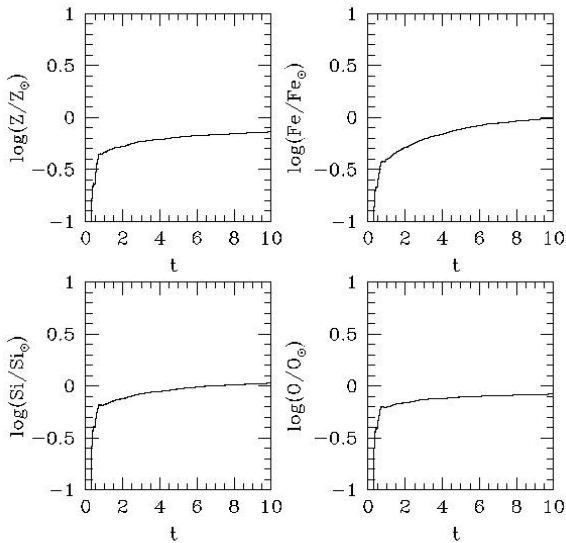
SN Type II

Chemical Enrichment: Metals

SA

SB

L



From left to right and from top to bottom:

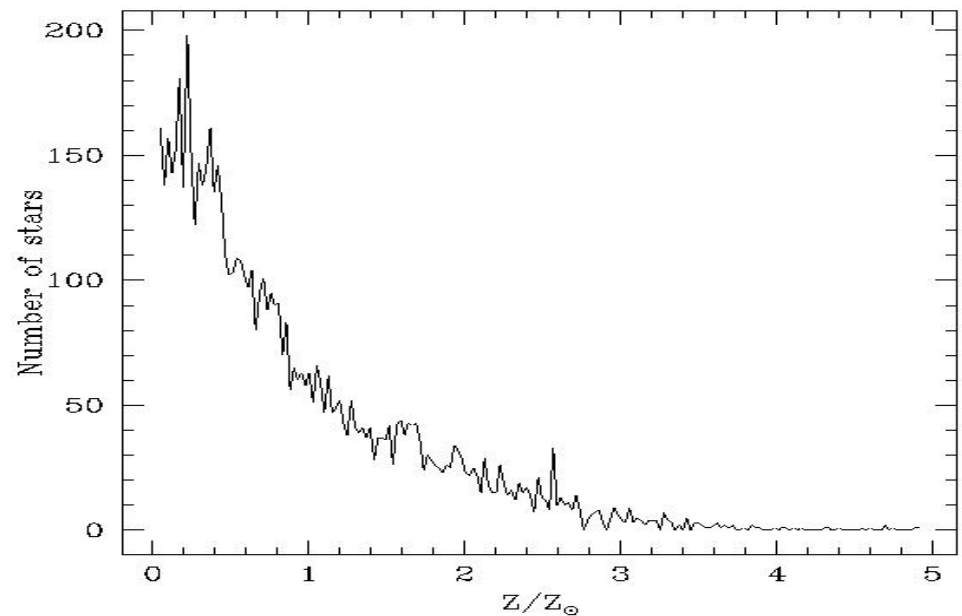
Z/Z_{\odot} , $\text{Fe}/\text{Fe}_{\odot}$, $\text{Si}/\text{Si}_{\odot}$, $\text{O}/\text{O}_{\odot}$

Metallicity Distribution among Stars

Model SA

71% stars with $Z < Z_{\odot}$
26% stars with $Z_{\odot} < Z < 3Z_{\odot}$
3% stars with $Z > 3Z_{\odot}$

UV Excess ?

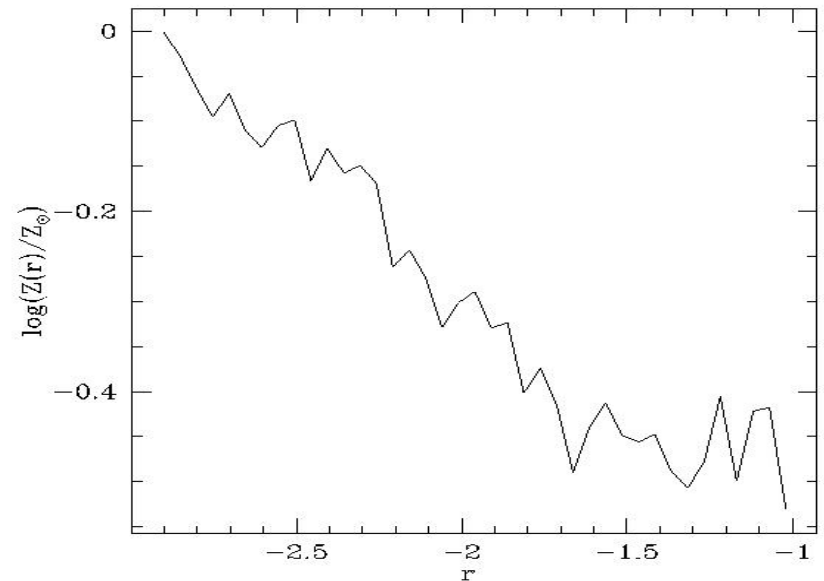


Metallicity Gradients

Model SA

Observed $\Delta \log Z / \Delta \log R = -0.2 \pm 0.1$
Davies et al (1993)

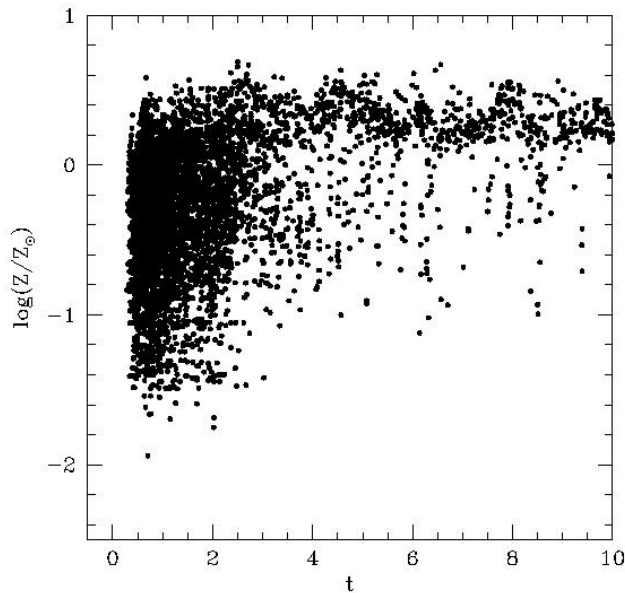
Calculated $\Delta \log Z / \Delta \log R = -0.3$



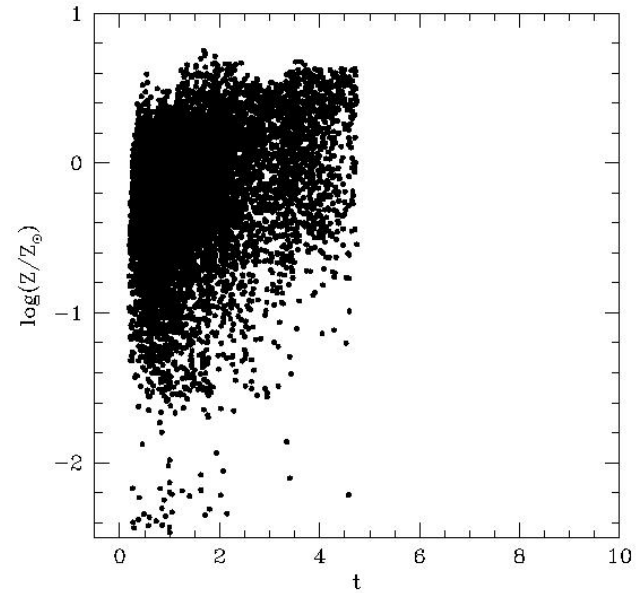
Radii in $\log R$ [Mpc]

Age-metallicity relationship

Model SA



Model SB



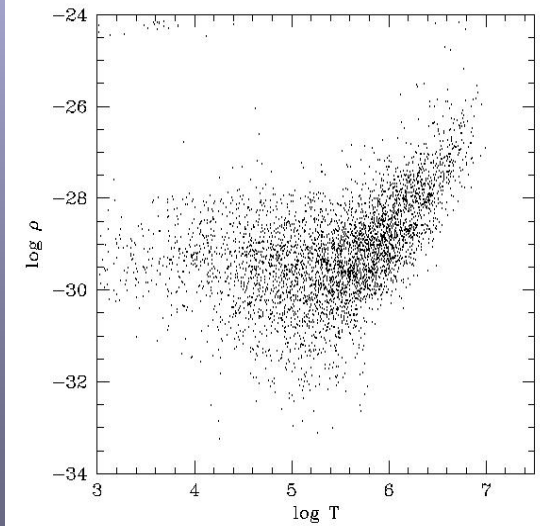
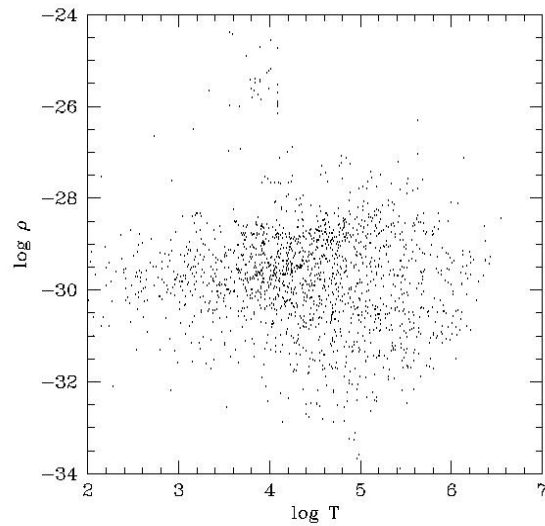
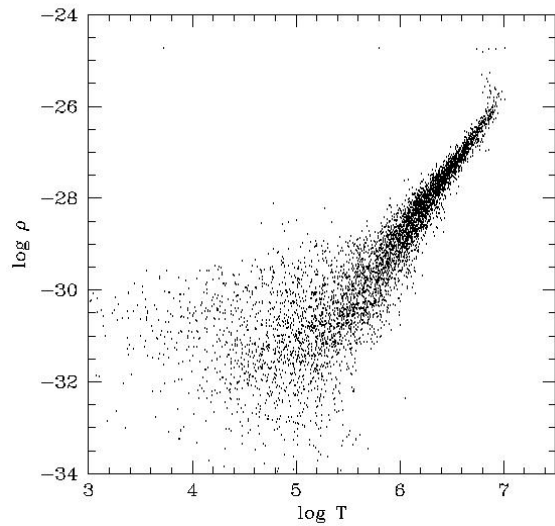
Ages in Gyr

Density vs Temperature of gas

SA

SB

L

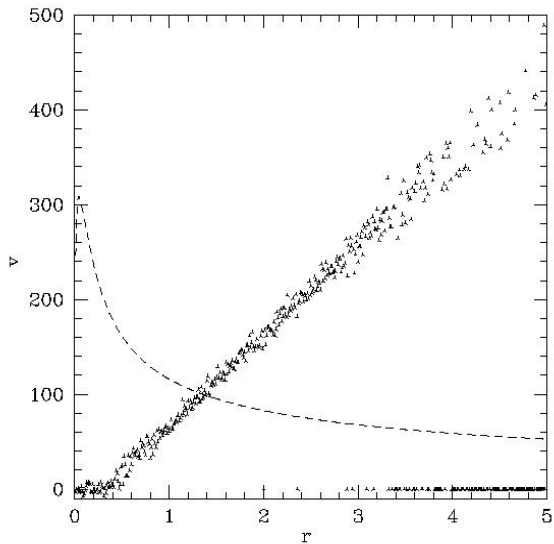


Galactic Winds

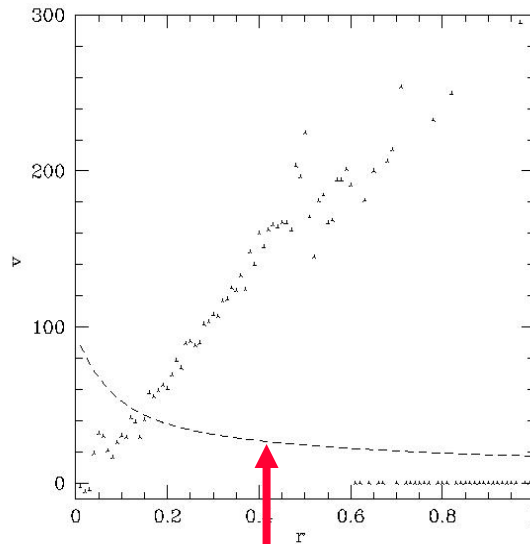
SA

SB

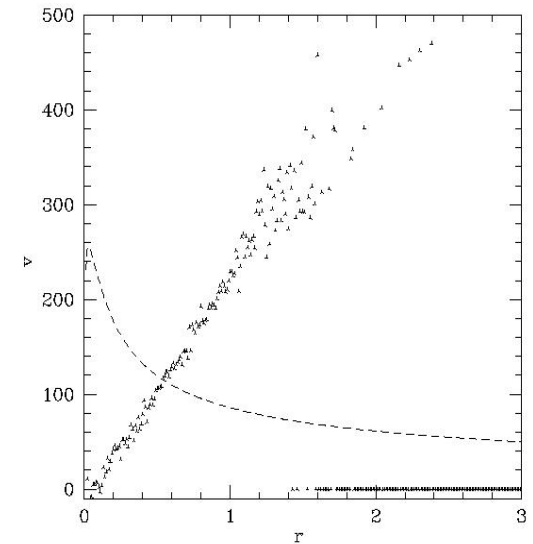
L



Velocities in km/s



V_{esc}



Distances in Mpc

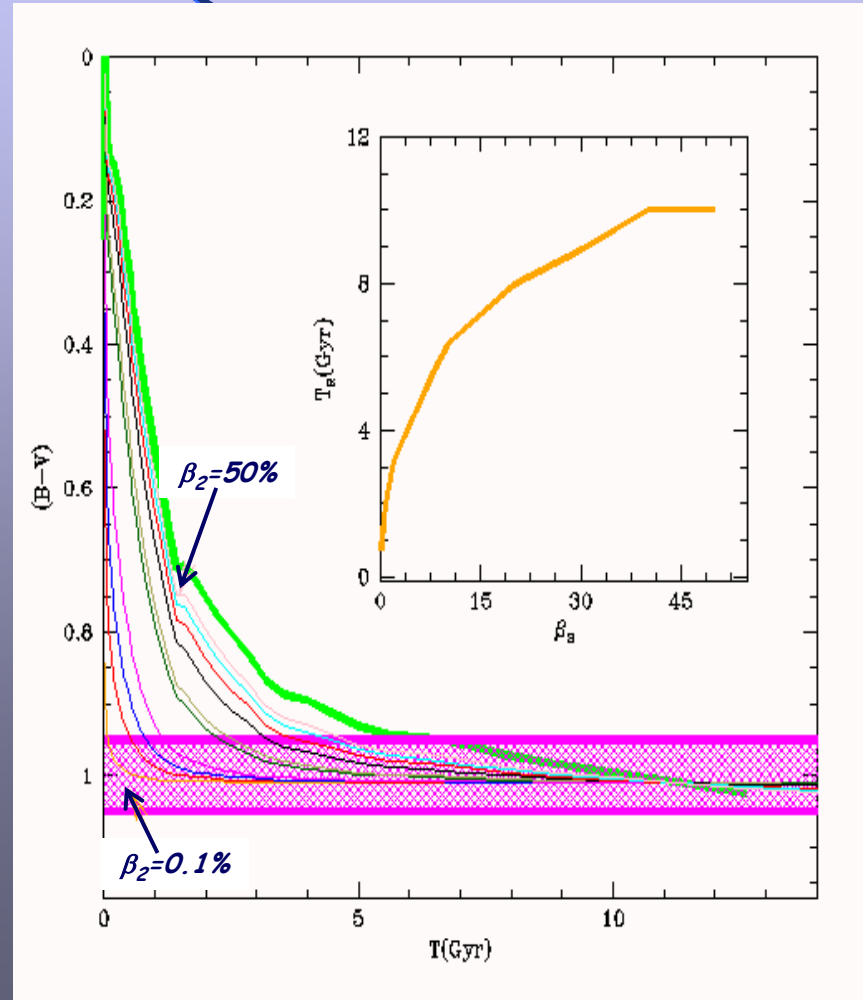
Conclusions

- All the models conform to the revised monolithic scheme, because mergers of sub-structures occurred early on
- Galaxy formation is complete at redshift $z=2$
- Structural properties, mean metallicity and metallicity gradients of present day models agree with current data
- Conspicuous galactic winds occur
- The duration of star formation seems to increase with decreasing total mass (see also Chiosi & Carraro 2002)
- The revised monolithic promises to be the right trail to follow in the forest of galaxy formation and evolution. See also Kawata (1999, 2001a,b), Kawata & Gibson (2003) and Kobayashi (2005)

Mergers? Yes but at least

- Several independent arguments and many observational hints (broad - band colors, indices etc..) seem to suggest that mergers (hierarchical scenario) are not the dominant mechanism by which galaxies (EGs) are assembled.

Mergers are spectacular events!



*Single prominent episode or
several bursts of star
formations?*

The gravitational pot

- Duty cycle:
...stars - energy generation -- gas heating - gas enriching - gas cooling - stars....
- The pot: gravitational potential well
- Therefore: total galaxy mass & initial density are the key parameters

Initial overdensity

$$\rho(z) = \bar{\rho}_0 \geq \rho_U(z)$$

$$\rho_U(z) = \frac{3h^2 \cdot 100^2}{8\pi G} (1+z)^3$$

$$\rho_U(z) = 1.99 \times 10^{-29} h^2 (1+z)^3 \text{ g/cm}^3$$

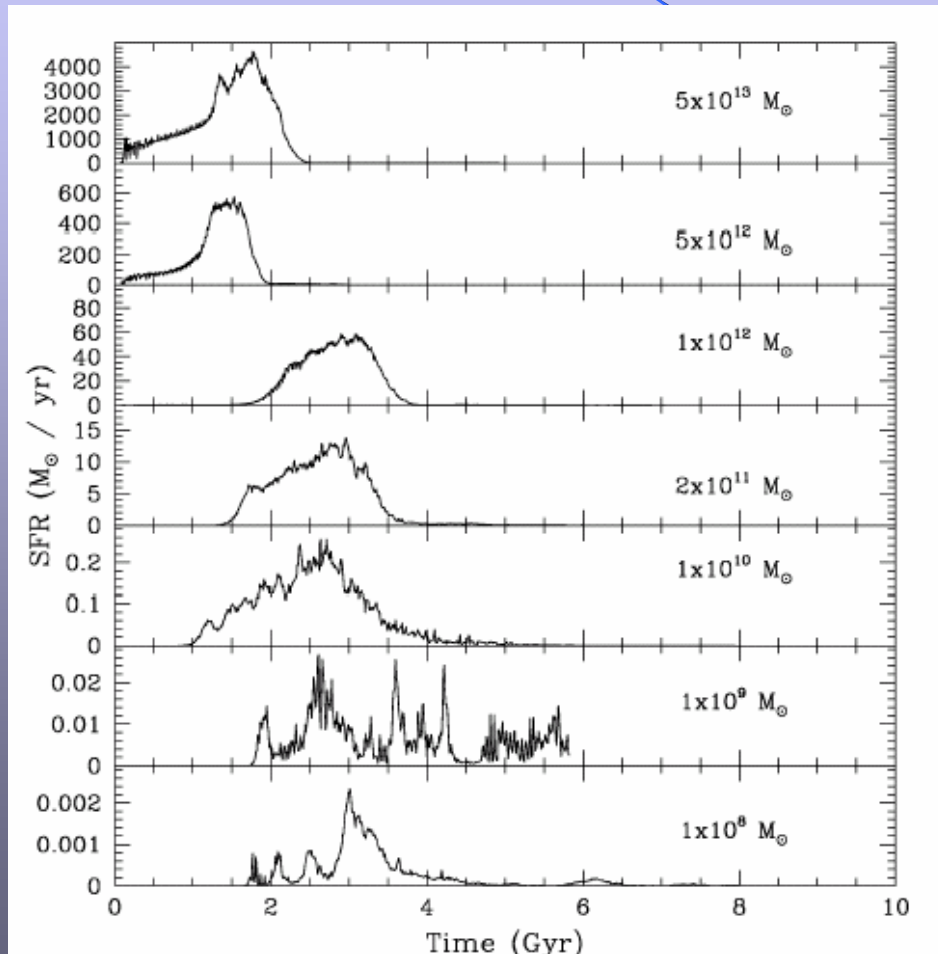
$$h = H / 100$$

Assumed total mass M_T derive

$$R_{200}(z) = \left(\frac{3}{4\pi}\right) \left(\frac{M_T}{200\rho_U(z)}\right)^{1/3}$$

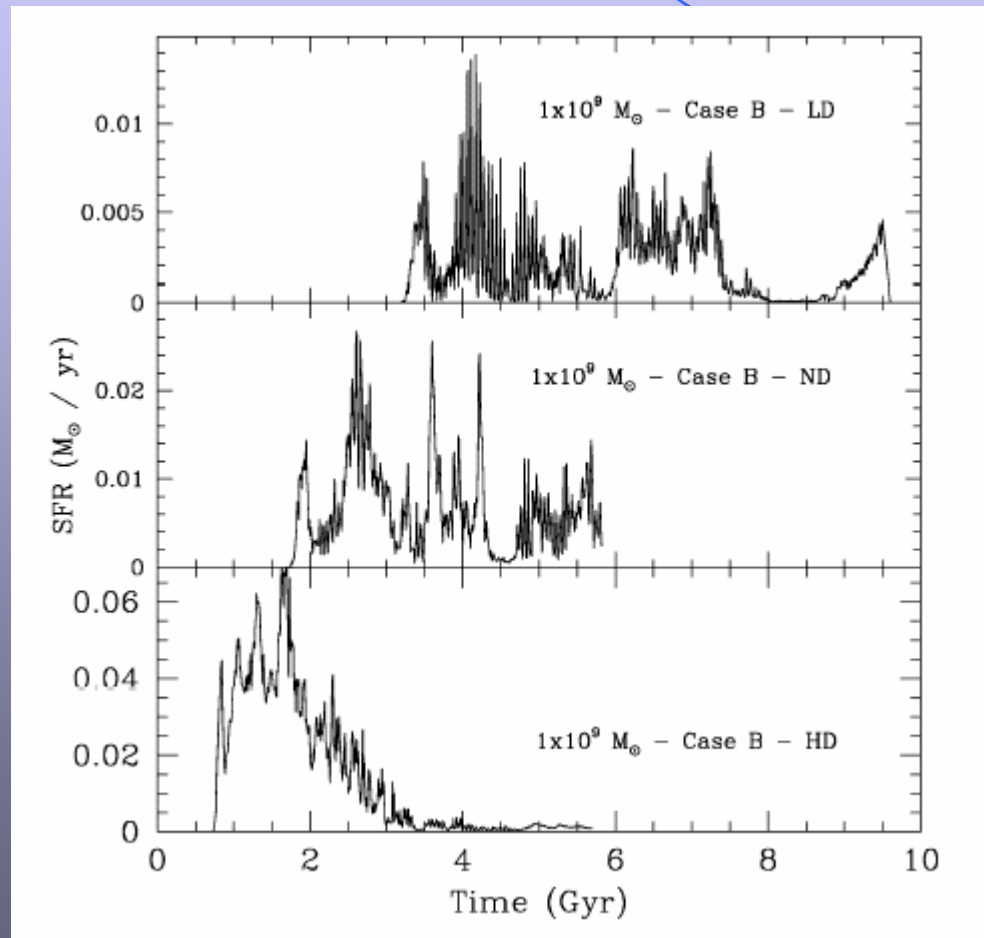
$$R_{200}(z) = 0.0967 \times 200^{-1/3} \left(\frac{M_T}{h^2}\right) (1+z)^{-1}$$

Same initial overdensity but different mass



Passing from monolithic to bursting mode at decreasing mass

Same mass but different initial overdensity



Passing from monolithic to bursting mode at increasing overdensity

Morphological evolution of dwarf galaxies in the local group

Pasetto, Chiosi & Carraro (2003, A&A 405, 931)

Carraro Chiosi, Lia & Girardi (2001, MNRAS 327, 69)

Aims and rationale

- Dwarf Galaxies (dG) in local group can be grouped in irregulars (dIrr), ellipticals (dE) and spheroidals (dSph)
- There seems to be a correlation between morphology and positions: dIrr more frequent in the outskirts, dE and dSph in the central regions
- Can dynamical interactions (tidal forces) with a dominant galaxy turn a dIrr into a dE or dSph?
- To answer the question is the aim of this study

A selected group of dGs with known kinematical parameters

Galaxy	l_{2000}	b_{2000}	D_{hel}	$\sigma_{D_{\text{hel}}}$	$V_{R_{\text{hel}}}$	$\sigma_{V_{R_{\text{hel}}}}$	μ_{α}	$\sigma_{\mu_{\alpha}}$	μ_{δ}	$\sigma_{\mu_{\delta}}$
	degrees		kpc		km s^{-1}		mas yr^{-1}			
Sculptor	287.5	-83.2	79.0	4	108	3	0.73	0.22	-0.07	0.25
Ursa Minor	105.0	44.8	69.4	4	-248	2	0.06	0.08	0.07	0.10
Draco	86.4	34.7	82.0	6	-293	2	0.60	0.40	1.10	0.50
Sagittarius	5.6	-14.1	24.0	2	140	5	-2.65	0.08	-0.88	0.08
LMC/SMC	282.0	-34.0	49.0	2	274	3	1.61	0.19	-0.06	0.25

in km/s

Components of the galactocentric
Velocity Vector:

V_x toward the Sun

V_y tangential to galactic rotation

V_z perpendicular to galactic plane

Galaxy	V_x	V_y	V_z
Sculptor	-218.6	+46.1	-243.4
Ursa Minor	+27.9	+74.1	-227.8
Draco	+422.2	+74.4	-195.9
Sagittarius	+204.7	+35.6	+281.3
LMC/SMC	+29	-63.7	-206.5

The probe galaxy to be launched in orbit

$$\rho_D(R, z) = \frac{M_D}{4\pi h^2 h_{z,D}} \exp\left(-\frac{R}{h_{R,D}}\right) \sec h^2\left(\frac{z}{h_{z,D}}\right)$$

where

M_D total disc mass,

$h_{R,D}$ radial scale length, $h_{z,D}$ vertical scale height

A small disk galaxy (the tightest configuration) simulating a dlrr

If a disk is affected by dynamical effects, then a dlrr is too !

$$\rho_H = \frac{M_H}{2\pi^{3/2}} \frac{\alpha}{r_c} \frac{\exp\left(-\frac{r^2}{r_c^2}\right)}{r^2 + \gamma^2}$$

$$\alpha = [1 - \sqrt{\pi} q \exp(q^2)(1 - \operatorname{erf}(q))]^{-1}$$

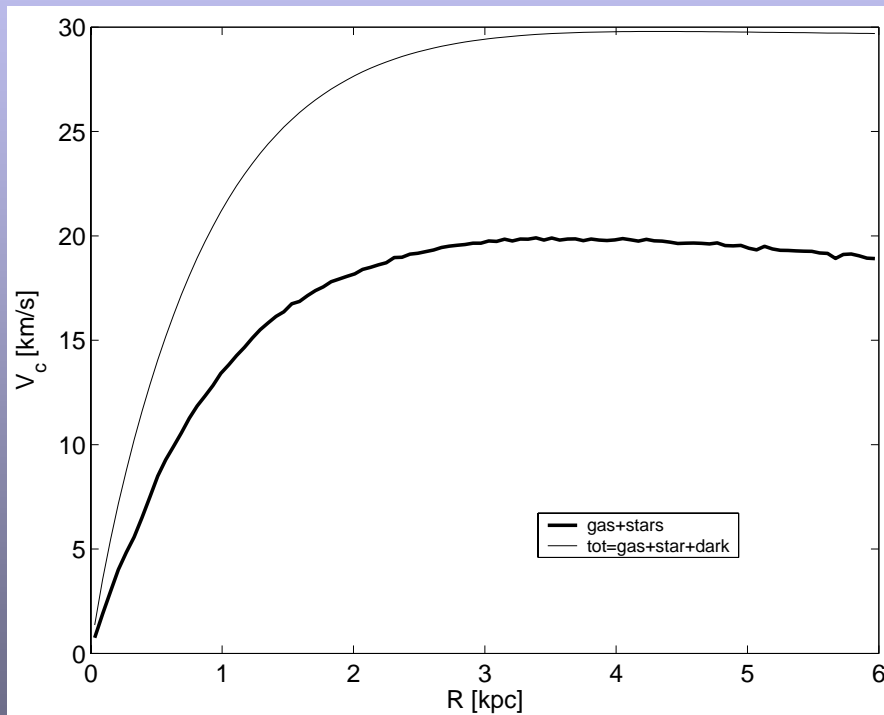
$$\gamma = 1 \text{ kpc}, \quad q = \gamma / r_c, \quad \text{and} \quad r_c = 6 \text{ kpc}$$

Initial parameter for the disk galaxy

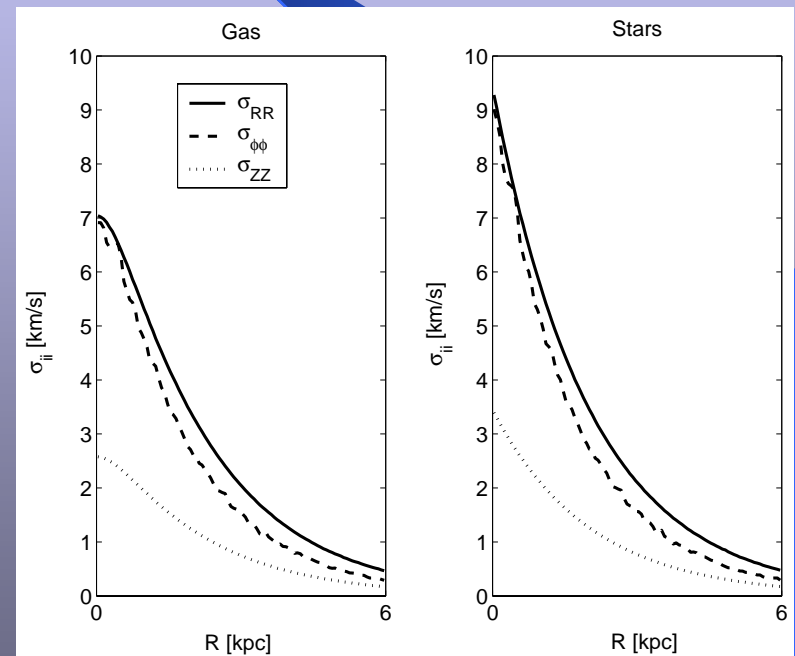
Masses ($10^7 M_\odot$)				Mass resolution ($10^4 M_\odot$)		
M_T	$M_{g,T}$	$M_{s,T}$	$M_{D,T}$	ΔM_g	ΔM_s	M_{DM}
49.0	2.45	2.45	44.1	0.49	0.49	6.30

Scale parameters (kpc)								
$h_{z,s}$	$z_{s,max}$	$h_{z,g}$	$z_{g,max}$	$R_{D,max,s}$	$R_{D,max,g}$	γ_H	r_c	$R_{H,max}$
0.100	1.000	0.020	0.900	6.000	6.000	1.000	6.000	12.000

Structure of a disk galaxy made of stars, gas and dark matter and evolved in isolation



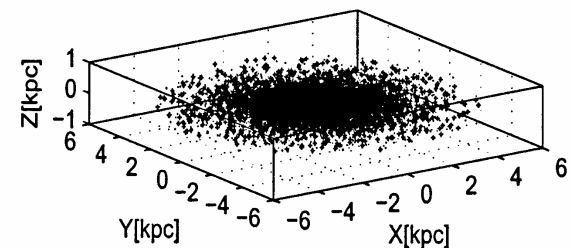
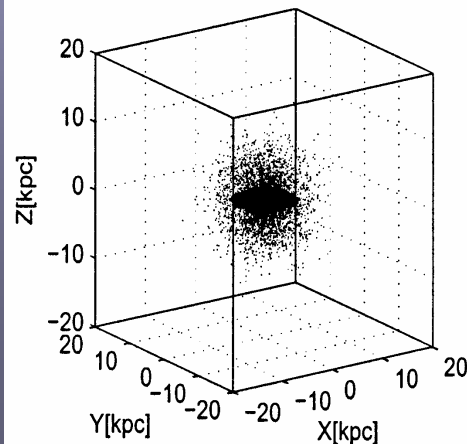
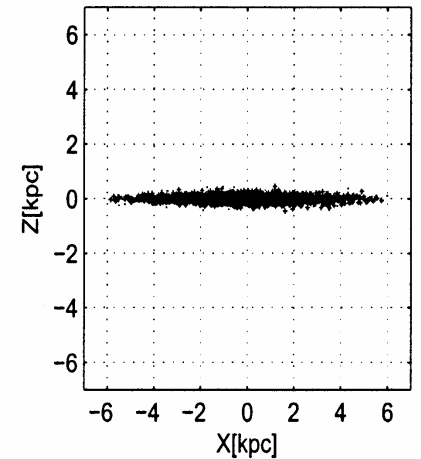
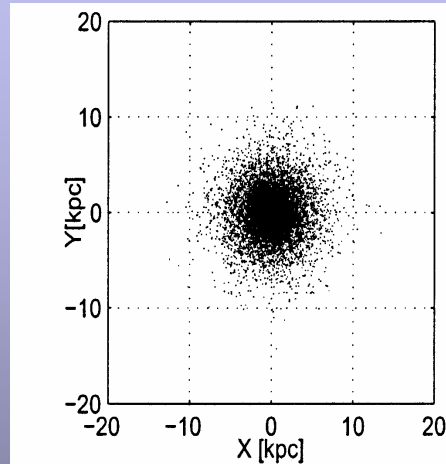
Radial profiles of circular velocities



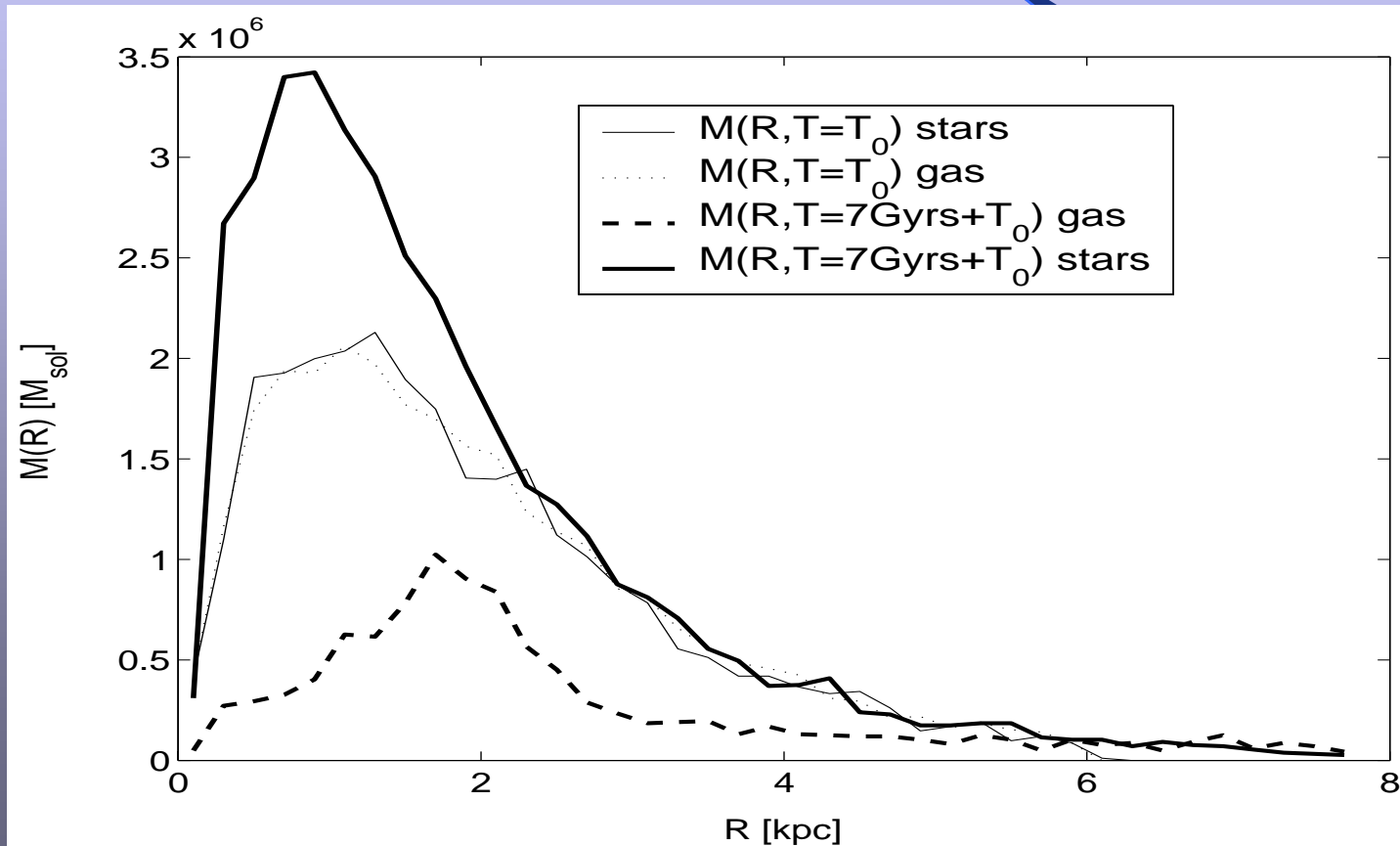
Radial profiles of the 3 components
of the velocity dispersion (gas & stars)

Structure of a disk galaxy made of stars, gas and dark matter and evolved in isolation

Beginning of the
simulation, i.e.
age T_0

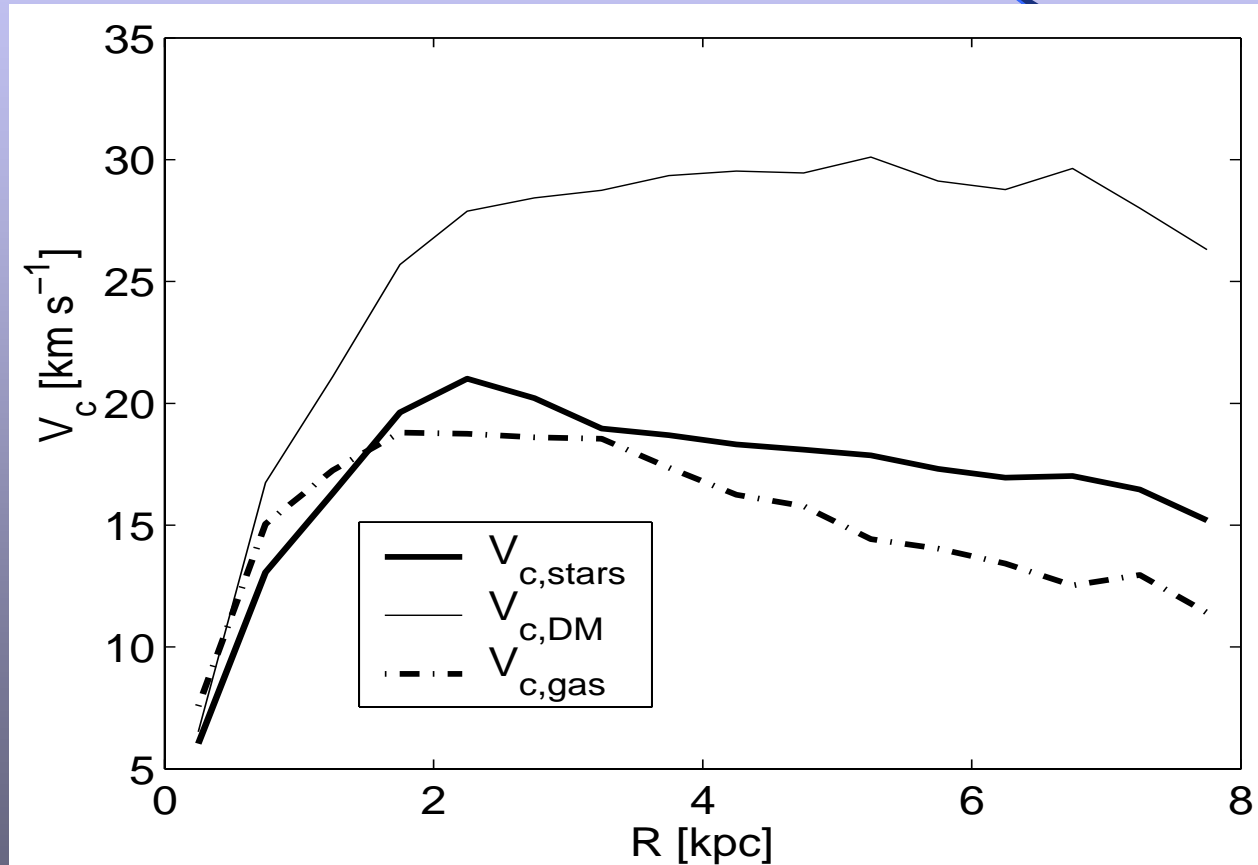


The test galaxy is a good one



The mass profile of the three components

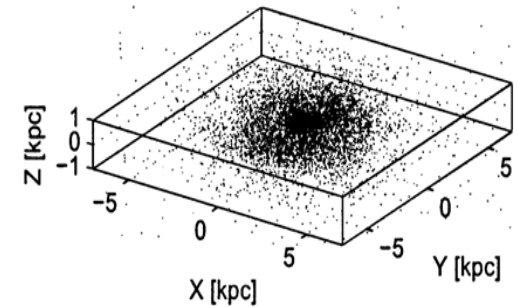
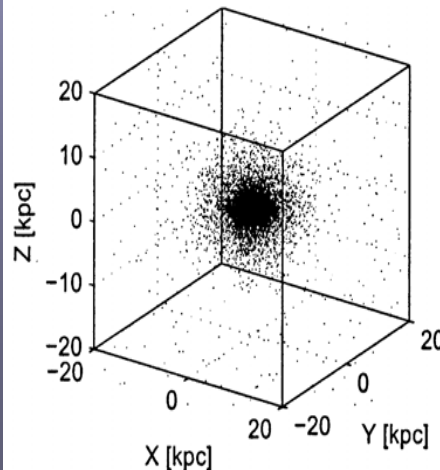
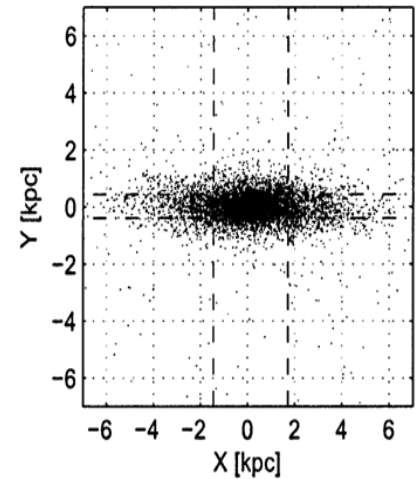
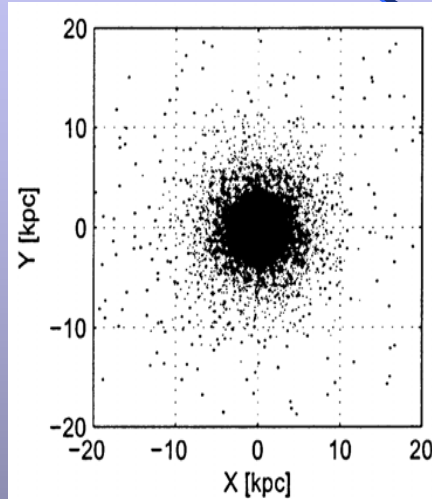
Mean radial profiles of circular velocities



For stars, gas and dark matter

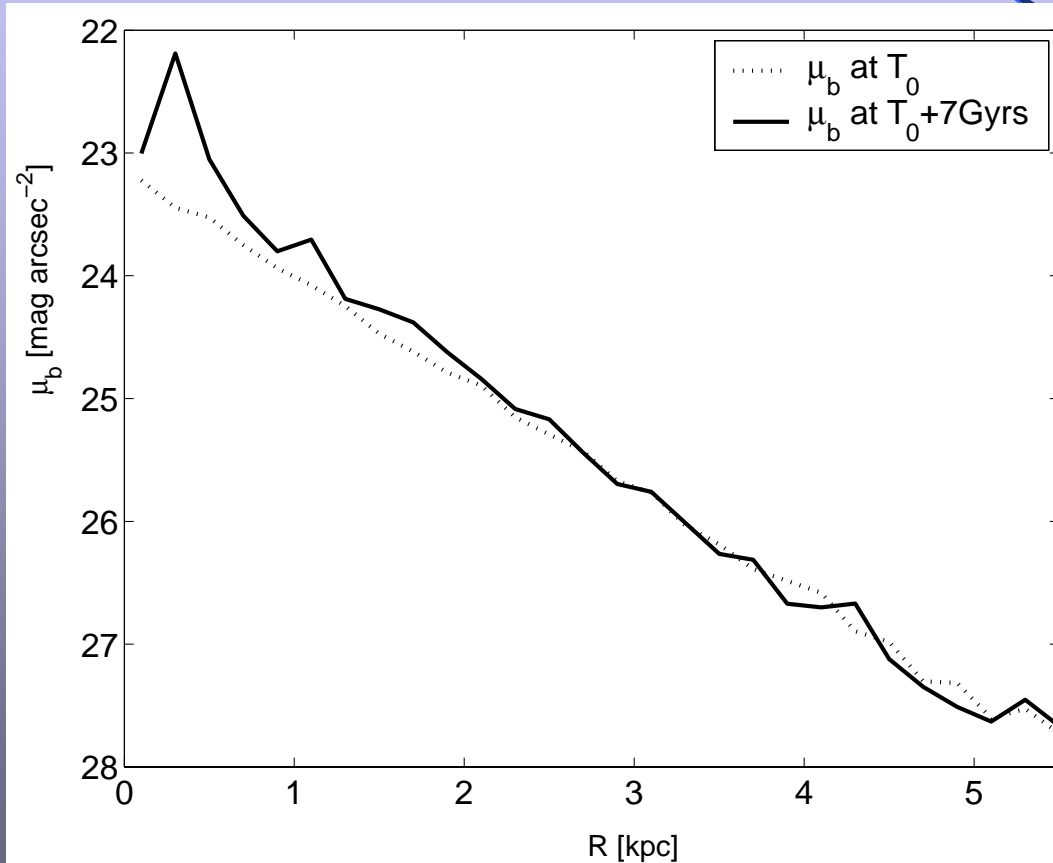
A picture taken much later....

Age $T_0 + 6$ Gyr



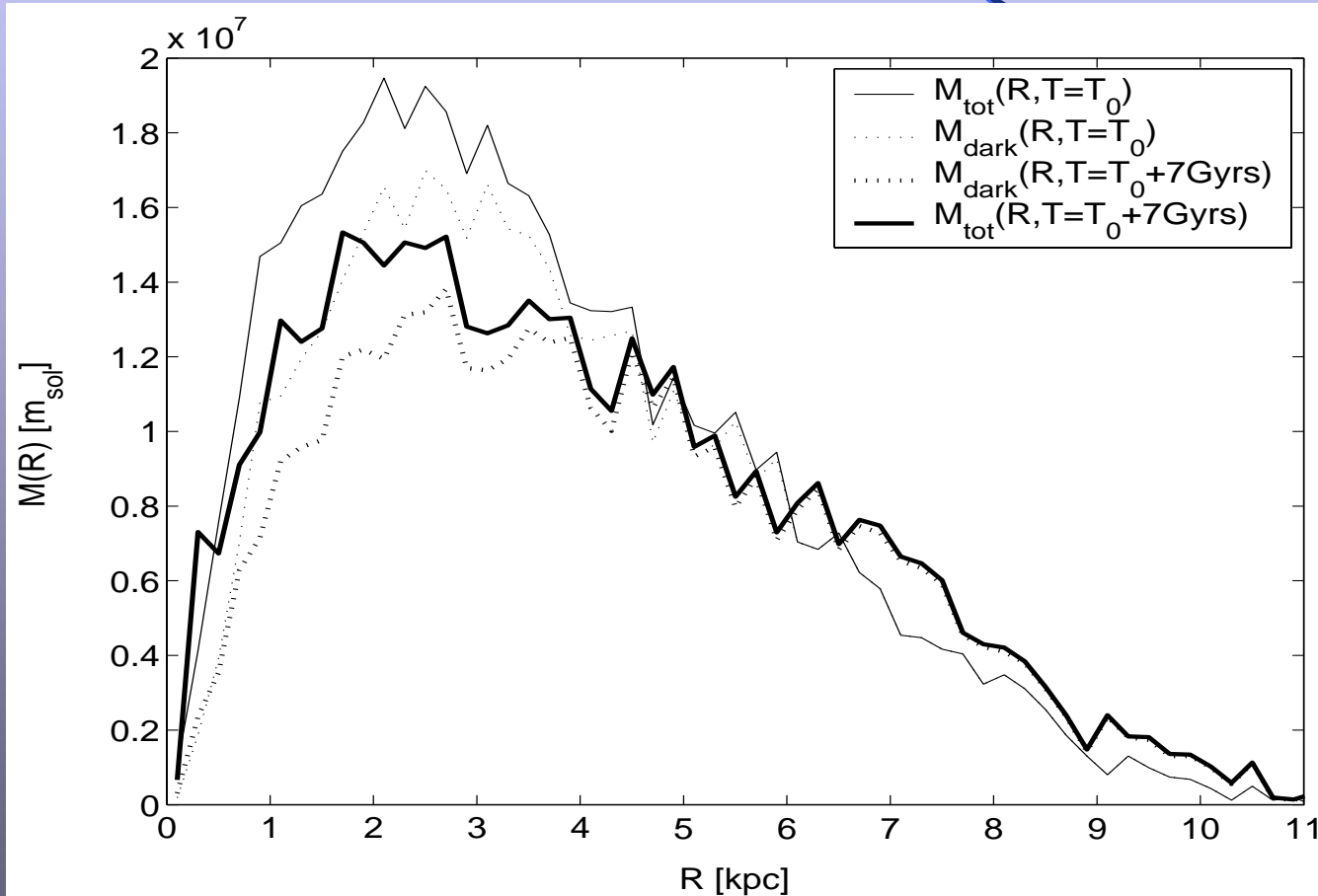
Note that the test Galaxy is still rather thin in z

Surface luminosity profiles



Two ages: T_0 and $T_0 + 7$ Gyr

Mass profiles (dark and total) at two ages



Masses in solar units

Plunge this galaxy onto an orbit around the Milky Way

- Define the gravitational potential of the Milky way made of
 - Halo
 - Disk
 - Neglect the Bulge

Gravitational potential of the MW: Halo

Halo: generated by the following distribution of mass

$$M_{HMW} = \frac{M_{HMW} \left(\frac{R}{R_{HMW}}\right)^\gamma}{1 + \left(\frac{R}{R_{HMW}}\right)^{\gamma-1}}$$

$$M_{HMW} = 1.07 \times 10^{11} M_\odot$$

$$R_{HMW} = 12 \text{ kpc}$$

$$\gamma = 2.02$$

$$\Phi(R) = -\frac{GM_{HMW}(R)}{R} - \frac{GM_{HMW}}{(\gamma-1)R_{HMW}} \times \left[-\frac{\gamma-1}{1 + \left(\frac{R}{R_{HMW}}\right)^{\gamma-1}} + \ln\left(1 + \frac{R}{R_{HMW}}\right) \right]^{\gamma-1} \Bigg|_R^{R_{HMW,T}}$$

Gravitational potential of the MW: Disk

$$\Phi = - \frac{GM_{DMW}}{\sqrt{R^2 + \left(R_{DMW} + \sqrt{z^2 + z_{DMW}^2} \right)^2}}$$

$$M_{DMW} = 8.56 \times 10^{10} M_{\odot}$$

$$R_{DMW} = 5.31 \text{ kpc}$$

$$z_{DMW}^2 = 0.25 \text{ kpc}$$

Choosing the satellite to analyze

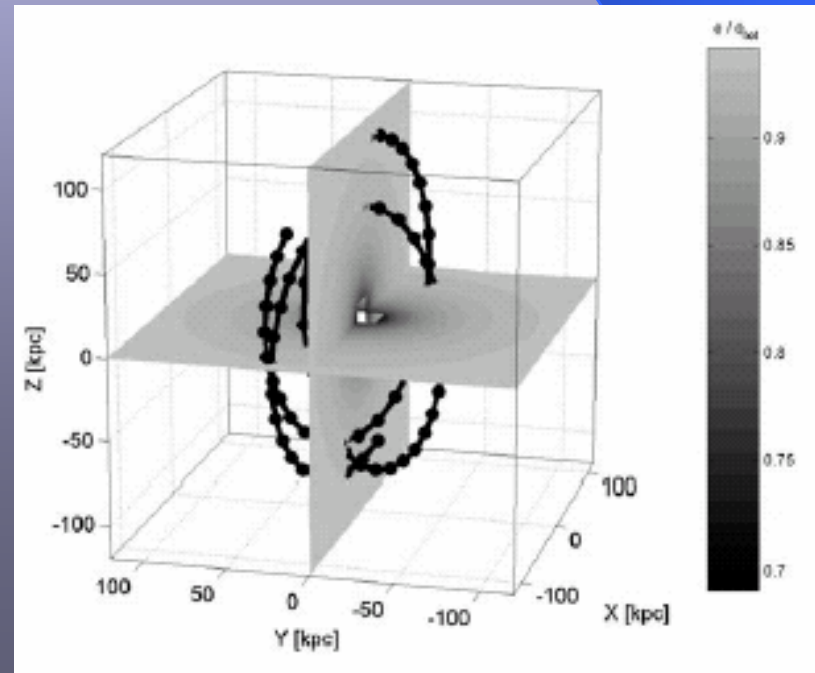
- For the purposes of this study:
- we have chosen *Sculptor*
- and calculated the orbit over about 8 Gyr after T_0 (time of launch)

3D view of the gravitational potential of MW + orbit dG

Represented by the scalar

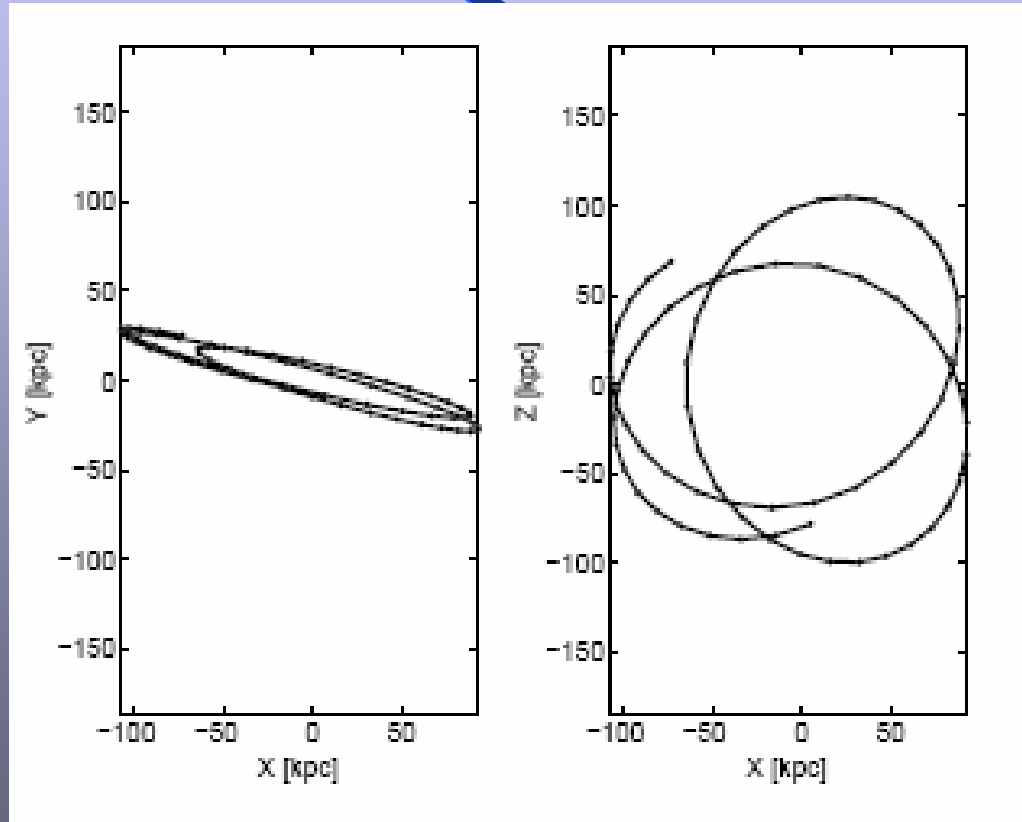
$$\Psi(X,Y,Z) = \frac{\Phi_{HMW}(X,Y,Z)}{\Phi_{HMW}(X,Y,Z) + \Phi_{DMW}(X,Y,Z)}$$

Satellite: Sculptor



Orbit of the satellite galaxy during 6 Gyr after T_0

Satellite: Sculptor



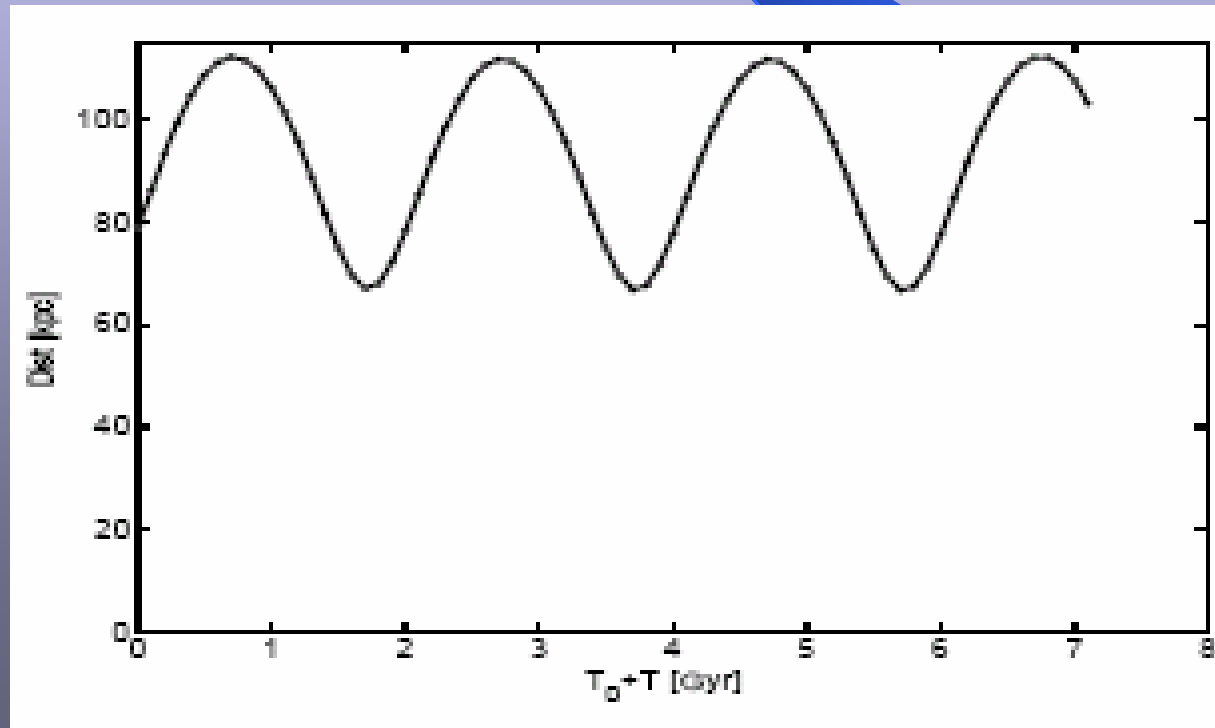
Orbit calculated from T_0 to $T_0 + 6$ Gyr

Distance of the satellite d_G to the MW during 6 Gyr after T_0

Satellite: Sculptor

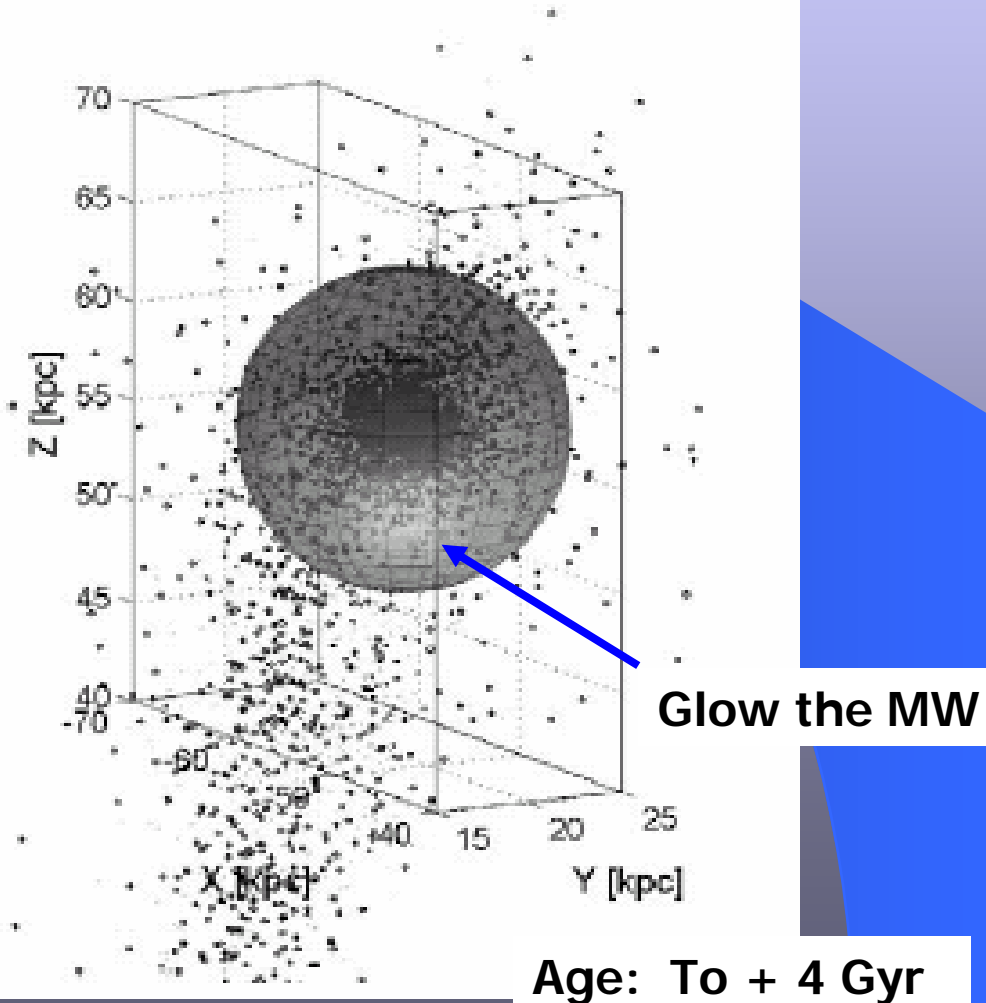
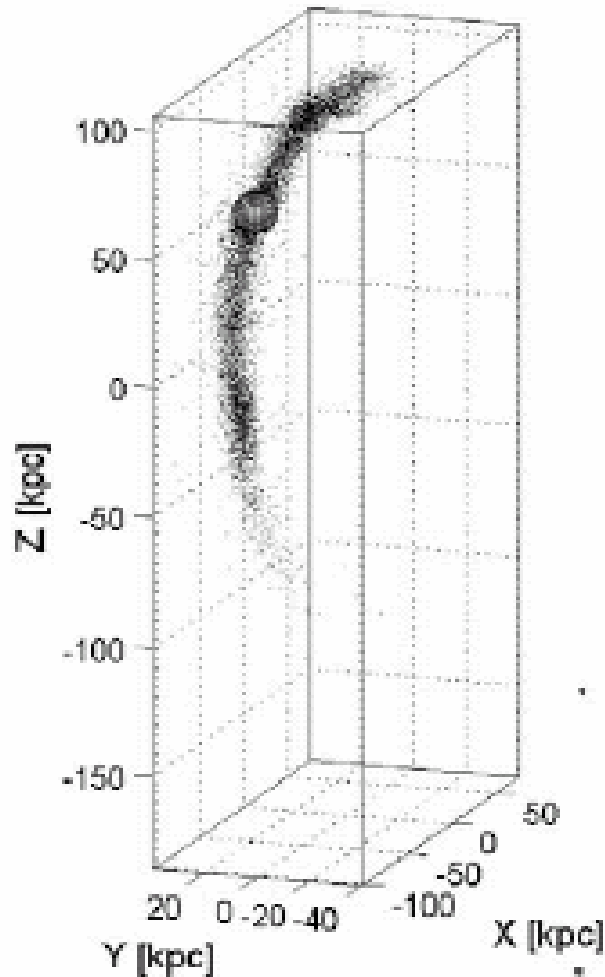
Apo-center 112 kpc

Peri-center 67 kpc

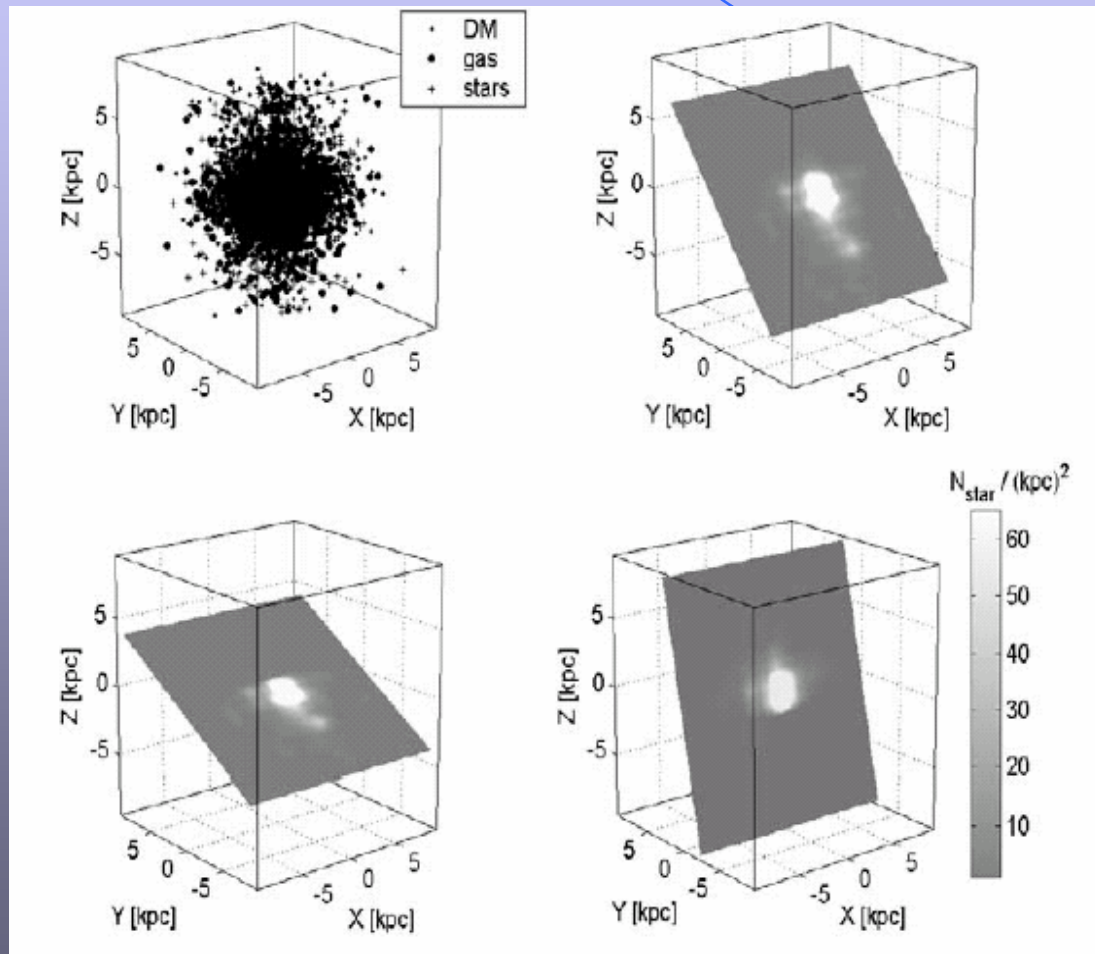


Orbital period: about 2 Gyr

Metamorphosis: $dIrr \rightarrow dSph$



3D view of the central region after 4 Gyr



It is nearly round indeed !

The dSph in numbers

Central body of the satellite at the age $T_0 + 4$ Gyr
(distances and dimensions in kpc)

Masses					Barycentre			Dimensions		
M_T	M_{bT}	$M_{d,T}$	$M_{d,T}$	$M_{SFR,T}$	X_B	Y_B	Z_B	ΔX	ΔY	ΔZ
1.31×10^8	8.06×10^6	4.55×10^7	7.78×10^7	1.39×10^7	-49.4	18.3	57.1	5.0	5.0	5.0

Central body of the satellite at the age $T_0 + 6$ Gyr

Masses					Barycentre			Dimensions			μ_B	V_c
M_T	M_{bT}	$M_{d,T}$	$M_{d,T}$	M_{NFS}	X_B	Y_B	Z_B	ΔX	ΔY	ΔZ	mag/as ²	km s ⁻¹
46.3	2.96	18.3	25.0	2.2	-49.4	18.3	57.1	4.0	3.8	3.9	≥ 22	≤ 4

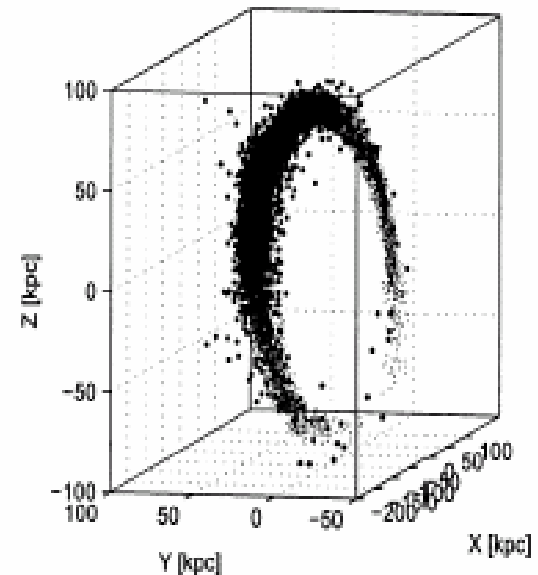
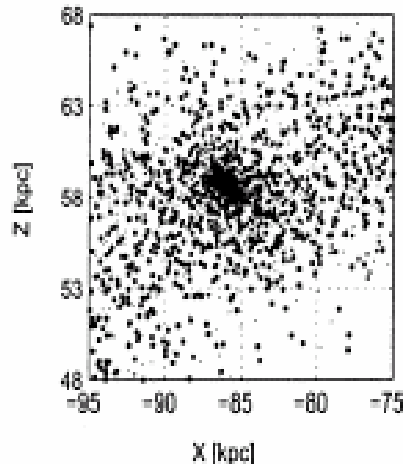
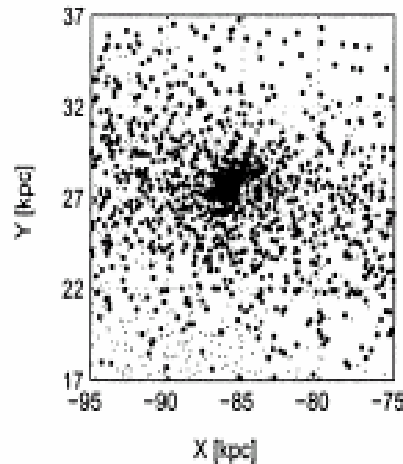
Masses in units of $10^6 M_\odot$

Main body of the satellite at $T_0 + 6$ Gyr

Ortographic projection
as seen from

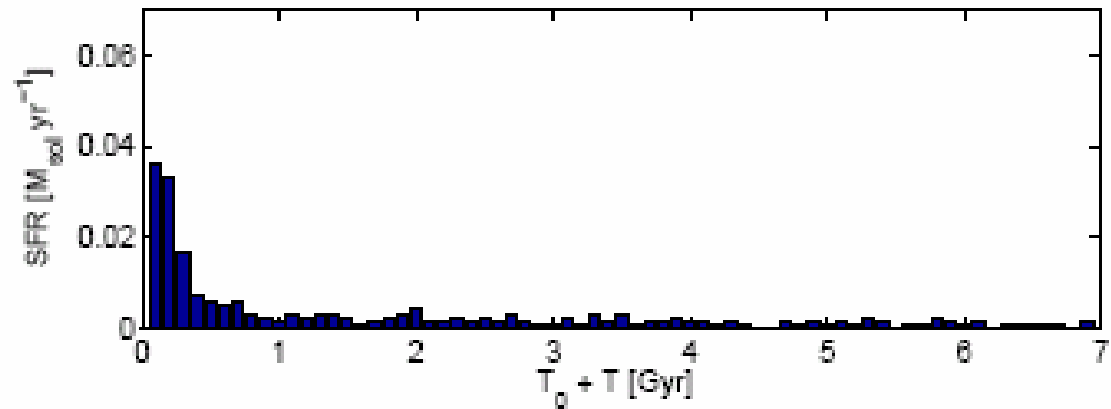
-69 azimuth
14 elevation

Note the remarkable tail
made of dark matter,
gas and stars

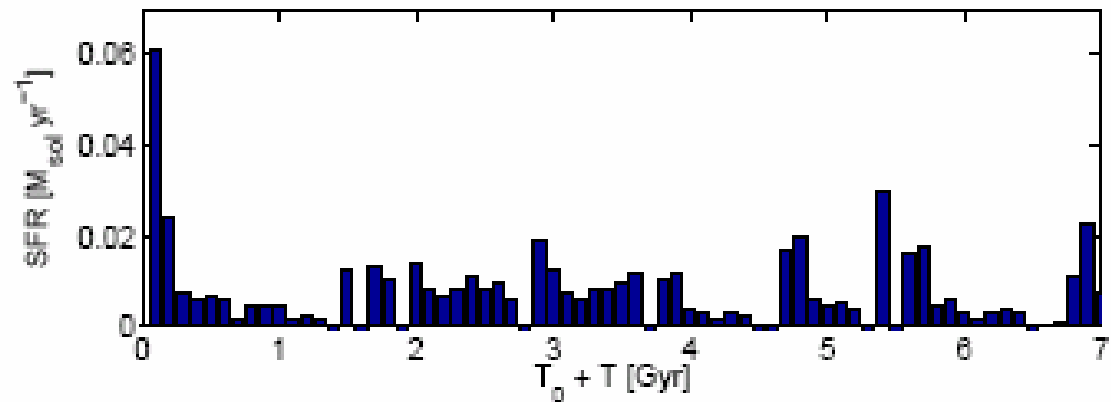


SFH: in isolation and in interaction

Isolation



Interacting

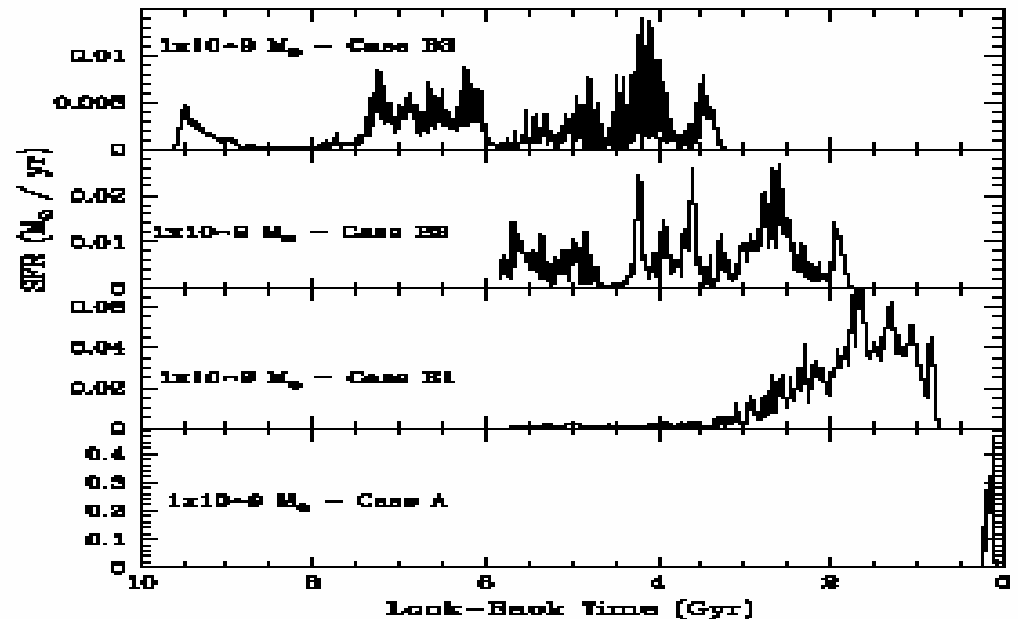


Note the bursts

Both isolated or interacting dwarf galaxies are likely to suffer the bursting mode of star formation with a large variety of individual histories

The mode of star formation is driven by the initial mean density of the galaxy.

At decreasing mean density it goes from initial spicke to many repated bursts.



Four models of different initial density and same M_T

Table 2. Initial conditions for the galaxy models.

Model	M_D $10^9 M_\odot$	M_B $10^9 M_\odot$	R_D kpc	ρ_b $M_\odot \text{kpc}^{-3}$
A	0.9	0.1	4	3.9×10^6
B1	0.9	0.1	16	5.8×10^4
B2	0.9	0.1	26	1.3×10^4
B3	0.9	0.1	35	5.5×10^3

Initial densities

Results

Table 3. Properties of the galaxy models.

Model	M_{star} $10^7 M_\odot$	M_{gas} $10^7 M_\odot$	$R_{c,B}$ kpc	σ_B km s^{-1}	σ_D km s^{-1}	$\rho_{c,B}$ $M_\odot \text{pc}^{-3}$	$\log(Z/Z_\odot)_{\text{Max}}$	$\log(Z/Z_\odot)_\psi$
A	3.2	6.8	0.07	10	25		-0.017	-1.158
B1	7.7	2.3	0.24	4.7	18.7	0.70	-0.128	-0.577
B2	2.5	7.5	1.55	6.2	15.2	0.09	-0.671	-1.079
B3	1.3	8.7	8.70	3.1	12.7	0.01	-1.032	-1.408

Choosing a certain cosmology to link rest-frame and cosmic ages

Table 5. T_G is the present age (in Gyr) of the Galaxy models. $T_{U, z_{\text{for}}}$ is the age of the Universe at the epoch of galaxy formation. H_0 is the Hubble constant in $\text{km s}^{-1} \text{Mpc}^{-1}$, whereas q_0 is the deceleration parameter. Finally z_{for} is the redshift at which galaxies are assumed to form.

H_0	q_0	z_{for}	T_G	$T_{U, z_{\text{for}}}$
50	0.	5	16.450	3.290
50	0.5	5	12.265	0.895
60	0.	5	13.708	2.742
60	0.5	5	10.220	0.746
70	0.	5	11.750	2.350
70	0.5	5	8.760	0.640

HRDs for model A

Prominent single burst of activity

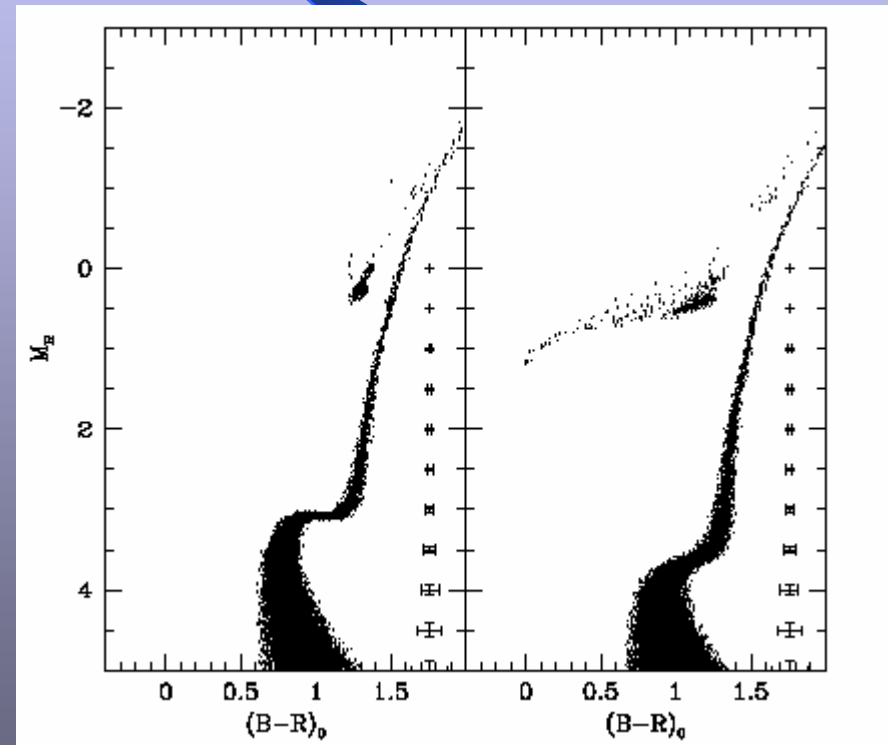
$\langle \log Z/Z_0 \rangle = -1.16$

Left

$H_0=70$, $q_0=0.5$ $z_{\text{for}}=5$ $T_G=8.76$ gyr

Right

$H_0=50$, $q_0=0$. $z_{\text{for}}=5$ $T_G=16.45$ gyr



It shows how the HRD of a Globular Cluster changes with the age

HRDs for model B1

Broad initial period of star formation

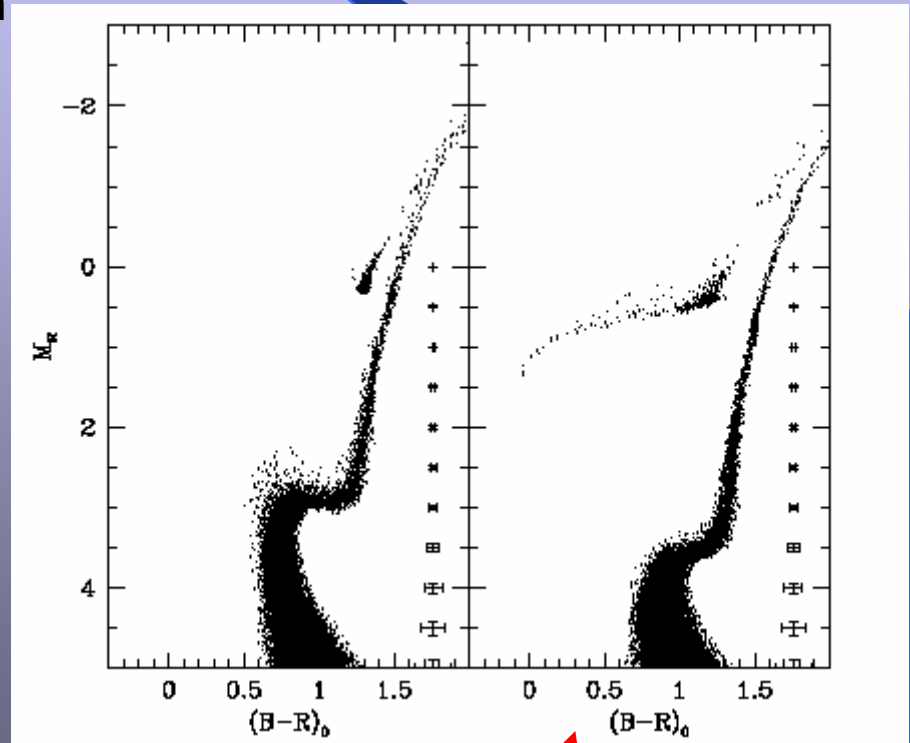
$$\langle \log Z/Z_0 \rangle = -0.58$$

Left

$$H_0 = 70, q_0 = 0.5, z_{\text{for}} = 5, T_G = 8.76 \text{ gyr}$$

Right

$$H_0 = 50, q_0 = 0, z_{\text{for}} = 5, T_G = 16.45 \text{ gyr}$$



Similar to model A but with some blurring due to age spread. They could mimic HRDs of Sculptor, Ursa Minor, Draco.....Leo II

HRDs for model B2

Several bursts of star formation

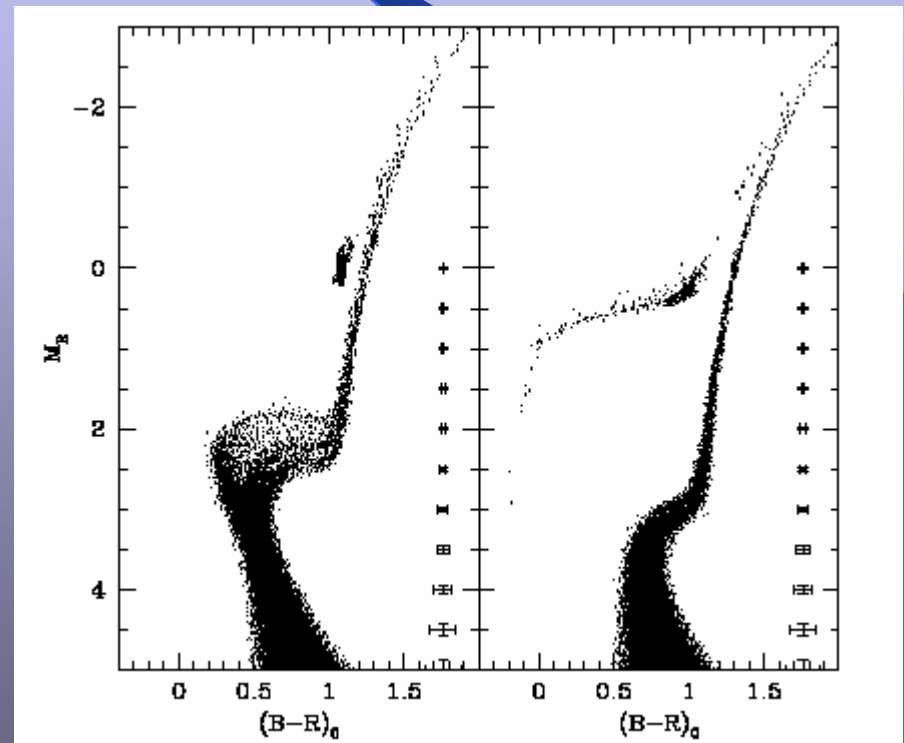
$$\langle \log Z/Z_0 \rangle = -1.08$$

Left

$$H_0=70, q_0=0.5, z_{\text{for}}=5, T_G=8.76 \text{ gyr}$$

Right

$$H_0=50, q_0=0, z_{\text{for}}=5, T_G=16.45 \text{ gyr}$$



The typical broad features of the HRD start to appear (at young ages)

HRDs for model B3

Many prolonged bursts of star formation

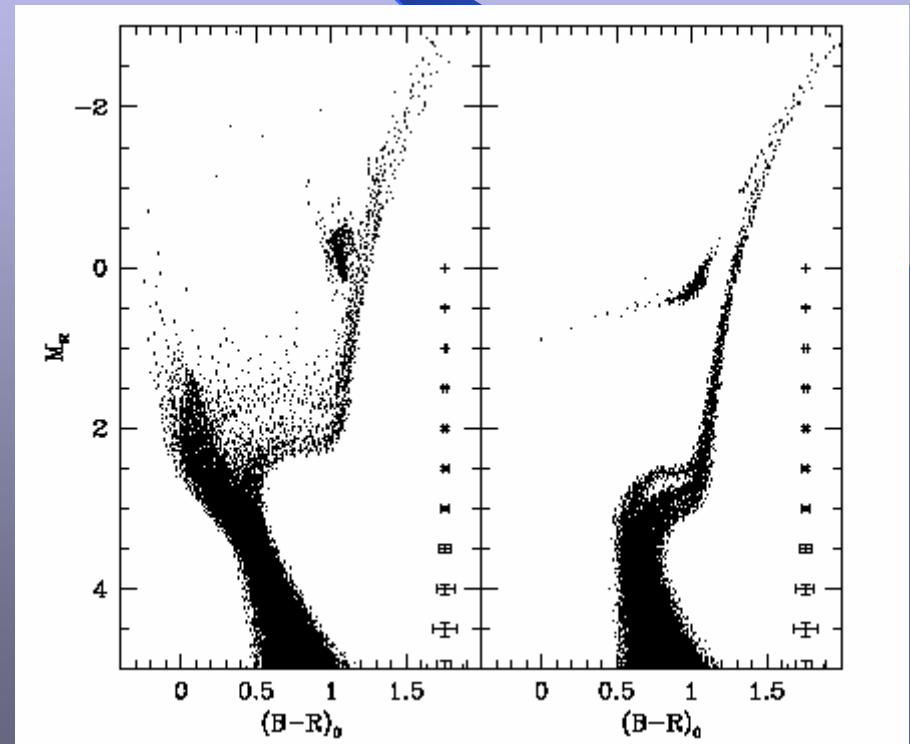
$$\langle \log Z/Z_0 \rangle = -1.48$$

Left

$$H_0=70, q_0=0.5 \quad z_{\text{for}}=5 \quad T_G=8.76 \text{ gyr}$$

Right

$$H_0=50, q_0=0. \quad z_{\text{for}}=5 \quad T_G=16.45 \text{ gyr}$$



Are these the analogs of Carina , Leo I ?

Conclusions

- Tidal interactions between a satellite and a host galaxy (MW for instance) may re-shape a dIrr into a dSph.
- The bursting mode of star formation is likely due to internal causes. However interactions (at close encounters) may enhance the star formation rate.